

Chapter 2

Heteropoly Compounds as Ammoxidation Catalysts

K. Narasimha Rao, Ch. Srilakshmi, K. Mohan Reddy,
B. Hari Babu, N. Lingaiah, and P.S. Sai Prasad

Contents

1	Introduction.....	12
1.1	Heteropoly Acids (HPAs) and Their Classification.....	13
1.2	Heteropoly Acids as Useful Catalysts.....	14
1.3	Modification of Heteropoly Acids.....	15
1.4	Salts of Heteropoly Acids and Their Catalytic Functionalities.....	16
1.5	Supported Salts of HPAs.....	16
1.6	In Situ Synthesis of AMPA.....	17
2	Experimental.....	19
2.1	Chemicals and Supports.....	19
2.2	Preparation of Various Types of HPA Catalysts.....	19
2.3	Characterization of HPAs.....	21
2.4	Ammoxidation of MP over HPA Salts.....	22
3	Results and Discussion.....	23
3.1	Studies on Bulk MPA and Vanadium Modified MPA (VMPA, VOMPA) Catalysts.....	23
3.2	Studies on TiO ₂ -Supported MPA, VMPA, and VOMPA.....	24
3.3	Studies on Bulk AMPA.....	26
3.4	Studies on AMPA Supported on Nb ₂ O ₅ , SiO ₂ , TiO ₂ , ZrO ₂ , and Al ₂ O ₃	35

K. Narasimha Rao
Chemistry Department, Faculty of Science, King Abdulaziz University,
P.O. Box 80203, Jeddah 21533, Saudi Arabia

Ch. Srilakshmi
Solid State and Structural Chemistry Unit, Indian Institute of Science,
Bangalore 560012, India

K. Mohan Reddy
Senior Research Associate, Center for Applied Catalysis, Seton Hall University,
South Orange, New Jersey 07079, USA

B. Hari Babu • N. Lingaiah • P.S. Sai Prasad (✉)
I & PC Division, Indian Institute of Chemical Technology, Hyderabad 500607, India
e-mail: pssaiprasad@gmail.com

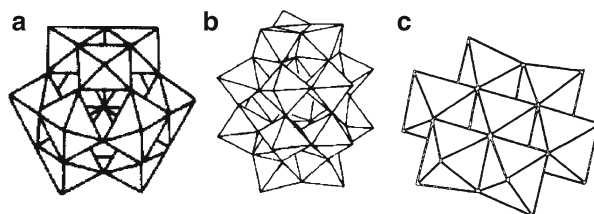
3.5	<i>In Situ</i> Synthesized AMPA-Based Systems	40
3.6	V, Sb, and Bi Modified AMPA-Based Systems	45
3.7	Supported Vanadium Incorporated AMPA Systems	47
4	Conclusions	52
	References	53

Abstract This chapter gives an overview of the work carried out in our group on the application of various forms of heteropoly acids (HPAs) for ammoxidation of methylpyrazine (MP). It starts with a general description of HPAs, ammonium salts of HPA, and the metal substituted HPAs (combinedly called as heteropoly compounds, HPCs). The various methods adopted for the synthesis of these compounds have been described. The HPCs have also been dispersed on different supports, and the methodology of their preparation is presented. Different characterization techniques have been used to determine their physicochemical properties. The reactivity of the catalysts is evaluated for the ammoxidation of 2-methylpyrazine (MP) to 2-cyanopyrazine (CP). The enhanced thermal stability and activity of the supported systems compared with those of the bulk ones are highlighted. Two new methods – one for the preparation of catalysts by *in situ* synthesis of the ammonium salt of heteropoly acid on supports and the other for the determination of dispersion of HPC on the support by FTIR technique – developed in our laboratory are introduced. Finally, correlations drawn between the activity and selectivity with the physicochemical properties of HPCs are presented.

1 Introduction

The fine chemical industry has experienced tremendous growth over the past few years due to the high demand for products like pharmaceuticals, pesticides, fragrances, flavoring, and food additives. The production of these products, which require stringent specifications, is definitely nontrivial. The stoichiometric organic synthesis, largely followed so far, leaves huge quantities of inorganic salts as byproducts whose disposal is a serious problem due to the keen environmental awareness and tightened regulations. Furthermore, the increased competition in industry has pushed the research and development activity on fine chemicals toward finding more cost-effective catalytic routes. One specific area that has a large impact on the environment protection is the utilization of solid HPCs as alternate catalysts for conventionally used reagents such as HF, H₂SO₄, etc. In the area of environmental pollution abatement [1], HPCs have recently been identified as very active catalysts. The acidic and redox functionalities of HPCs are used in solution as well as in the solid state [2]. Heteropoly acids are well-known green catalysts for oxidation [3] and acid-catalyzed reactions [4]. The salts of heteropoly acids are more thermally stable than their parent acids [5] and are extensively used as catalysts to obviate solubility problems during the reactions. Many developments like incorporation of heteropoly acids into the channels of mesoporous materials have also been adopted

Fig. 2.1 Structures of heteropoly ion (a) Keggin, (b) Wells-Dawson, and (c) Anderson [8]



for improving product selectivity. There are still many areas for which new methods have to be explored. In this direction, concerted efforts have been directed toward developing more efficient HPC-based catalysts to be used in ammoxidation of aromatic and heteroaromatic compounds to their corresponding nitriles.

Single-step vapor-phase ammoxidation of different alkyl aromatics and heteroaromatics to their corresponding nitriles has become the topic of extensive research in recent times due to its usefulness as an essential commercial method. Selective synthesis of CP from MP by means of gas-phase ammoxidation is of particular industrial importance, because the resulting nitrile is a valuable intermediate for the production of an effective antitubercular drug, pyrazinamide. Pyrazinamide is a prodrug that stops the growth of *Mycobacterium tuberculosis*. Pyrazinamide is generally used in combination with other drugs such as isoniazid and rifampicin in the treatment of *Mycobacterium tuberculosis*. Initially, vanadia-based solids, either alone or in combination with other metals like Bi, Sb, and Nb particularly supported on TiO_2 [6], were used in the ammoxidation. However, all these catalysts were found to be active at high reaction temperatures ($>430^\circ\text{C}$) where the unwanted and more exothermic ammonia oxidation is favorable. Effective control of the exothermic reaction temperature is very critical, since there is every chance for reactor run away. Besides, in an exothermic reaction like that of ammoxidation, high reaction temperature always leads to drastic decrease in product selectivity. Efforts have been consistently made to develop low-temperature active catalysts. HPAs (e.g., 12-molybdophosphoric acid) and their ammonium salts are being viewed as promising low-temperature ammoxidation catalysts [7]. However, the low thermal stability of the bulk HPCs has become the major constraint for their applicability for vapor-phase reactions. Thus, efforts to develop novel catalyst systems with improved stability have become imminent.

1.1 Heteropoly Acids (HPAs) and Their Classification

The HPAs or polyoxometalates are made of a central or heteroatom linked with groups of peripheral atoms, again interlinked with oxygen atoms. These polyanions, having well-defined nanometer size structures, are classified based on the ratio between the polyatom and the heteroatom present in the total structure and the nature of arrangement of these atoms. These arrangements are classified mainly as Keggin, Well-Dawson, and Anderson structures [8]. The corresponding structures of heteropoly ions are shown in Fig. 2.1.

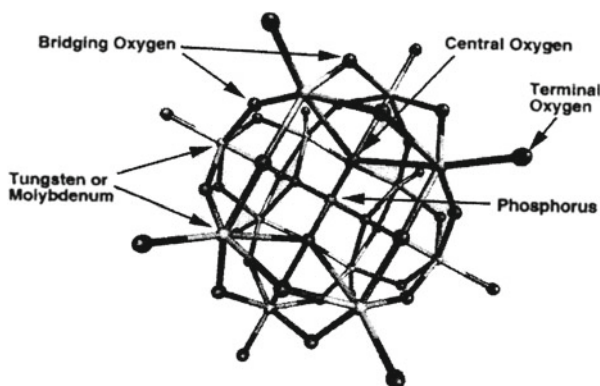


Fig. 2.2 The Keggin unit is the primary structure of the heteropoly acids and contains 12 transition metal atoms normally of tungsten or molybdenum, a central atom (usually phosphorus or silicon), and four types of oxygen atoms: central oxygens, terminal oxygens, and two types of bridging oxygens [3]

Among these compounds and their salts, those exhibiting Keggin-type polyanion structure are most extensively studied. The Keggin structures described by the general formula $H_nXM_{12}O_{40}$ ($M/X=12$) are also the most effective catalysts due to the unique combination of their stability, acidity, and structural accessibility. The central atom, X, is usually either P^{5+} or Si^{4+} , and the heteroatom, M, is usually W^{6+} or Mo^{6+} . The molecular Keggin structure consists of a central tetrahedron (XO_4^{n-}) surrounded by 12 linked octahedra containing the addenda atoms ($M_{12}O_{36}$). More than 65 elements from all groups of the periodic table can be found incorporated as heteroatoms [9].

Hereafter, the discussion in this chapter will be restricted to Keggin structures. As depicted in Fig. 2.2, there are four types of oxygen atoms in the Keggin unit: the central oxygen atoms (O_a), corner-sharing bridging oxygen atoms (O_b), edge-sharing bridging oxygen atoms (O_c), and terminal oxygen atoms (O_d). The central oxygen connects the heteroatom to a transition metal atom. The next two types of oxygen atoms bridge two transition metal atoms in adjoining octahedra. Finally, the terminal oxygen atom is bonded to only one transition metal atom [9]. The overall charge of the central tetrahedron is delocalized over the entire structure. Protons associate themselves with the exterior oxygen atoms (O_b , O_c , and O_d) and form acidic hydroxyl groups.

1.2 Heteropoly Acids as Useful Catalysts

The molybdo- and tungstophosphoric acids are found to be highly effective in catalyzing many reactions like olefin hydration and conversion of methanol to hydrocarbons [9]. Of late, the heteropoly acids are finding applications in the synthesis of fine chemicals too. They have also been widely involved in

heterogeneous catalytic oxidation processes such as commercial vapor-phase oxidation of methacrolein, which produces more than 80,000 tons of methacrylic acid per year [10]. The bifunctional HPA catalysts can be used for sequential hydroformylation and oxidation of olefins [11]. HPAs also display catalytic activity in water splitting and oxygen transfer to alkanes [12]. The oxidation of alkenes and the coupling of aromatics utilize molybdovanadates as the reoxidants in the Wacker process [13]. Catalysts containing polyoxomolybdates are widely used for hydrodesulfurization, hydrodenitrification of fossil fuels [14]. The commercially successful direct oxidation of ethylene to acetic acid utilizes palladium and a HPC as catalysts producing 100,000 tons/year of the product [15]. There is another rapidly growing area, which is the heteropoly compound photochemistry and photocatalysis. Recently, their usefulness in bleaching wood pulp via oxidative delignification has been reported [16]. Molybdenum-based heteropoly compounds are better catalysts for oxidation reactions than their tungsten counterparts. Other applications of HPAs as ion-exchange materials, ion-selective membranes, and inorganic resistant materials have also been reported [17]. Thus, there has been a vigorous research activity taking place on expanding the applications of HPCs.

1.3 *Modification of Heteropoly Acids*

As stated earlier, the Keggin-type heteropoly acids are known to possess the unique features of strong intrinsic acidity and oxidizing property. Both the features can be suitably modified, by the variation of the cationic composition as well as by substitution of a few atoms of either molybdenum or tungsten in peripheral positions in the anion with other transition metals such as V, Sb, Fe, and Ti [3, 18]. Roch et al. [19] studied the addition of transition metals to HPAs as an important approach to control their redox properties and to impart higher thermal stability. Conclusions are drawn based on the studies of catalyzed oxidative dehydrogenation of isobutyric acid by $\text{H}_4[\text{PMo}_{11}\text{VO}_{40}]$ and $\text{VOH}[\text{PMo}_{12}\text{O}_{40}]$ at 320 °C. Thermal treatment of $\text{H}_4[\text{PMo}_{11}\text{VO}_{40}]$ at 320 °C leads to a complex mixture of different species with or without vanadium inside the Keggin structure. It has been reported that the protonic form, $\text{H}_3\text{PMo}_{12}\text{O}_{40}$, catalyzes oxidation of lower alkanes and that substitution of V^{5+} for Mo^{6+} improves the catalytic activity and selectivity [12]. Iron and copper have been the most widely used additives for enhancing the catalytic activity of HPAs, as reported in the literature [20]. Among the transition metals, the effect of metals like vanadium, iron, zinc, chromium, and nickel, in both cationic and anionic positions, on the catalytic performance of heteropoly compounds in gas-phase oxidations has been studied [21]. Catalysts containing V in combination with these elements are known to be effective for the ammoxidation of hydrocarbon reactions [21]. The addition of vanadium to a heteropoly compound improves its catalytic functionality with respect to partial oxidations as well.

Vanadium incorporated molybdophosphoric acid catalyst shows a unique bifunctional property, which arises due to the redox nature of vanadium and the acidic character of the molybdophosphoric acid [22]. The molybdovanadophosphoric acid-based catalysts are used commercially for the synthesis of methacrolein and in the conversion of isobutyric acid to methacrylic acid. Ressler et al. [23] studied the bulk structural evolution of a vanadium-containing heteropolyoxomolybdate [$\text{H}_4(\text{PVMo}_{11}\text{O}_{40}) \cdot 13\text{H}_2\text{O}$], with vanadium substituting for Mo in the Keggin ion. Several authors have investigated molybdophosphoric acid (MPA) by replacing 1–3 Mo atoms with the corresponding number of V atoms [24, 25]. The main observation in the high vanadium incorporated systems is the expulsion of vanadium from the secondary structure and formation of a vanadyl (VO^{2+}) salt during catalysis [26]. Kozhevnikov [27] studied the applications of 40 Keggin-type heteropolyanions $\text{PMo}_{12-n}\text{V}_n\text{O}^{(3+n)-}$ as catalysts for aerobic liquid-phase oxidation.

1.4 Salts of Heteropoly Acids and Their Catalytic Functionalities

Berzelius [28] first synthesized ammonium phosphomolybdate in 1826, which is now known as ammonium 12-molybdophosphate. Because the salts of heteropoly acids possess higher thermal stability, higher microporosity, and insolubility in several solvents relative to the pure acid, ammonium salts of HPAs are used as catalysts for several high-temperature gas-phase reactions. Ammonium salt of 12-molybdophosphoric acid (AMPA), exhibiting the Keggin structure, has been studied for the oxidative dehydrogenation of isobutyric acid to methacrylic acid by McGarvey and Moffat [29]. The arrangement of NH_4^+ ion in heteropoly acid salt is shown in Fig. 2.3.

1.5 Supported Salts of HPAs

Initial catalytic studies were restricted to unsupported acids and their salts. However, as the bulk compounds had low surface area and inadequate thermal stability, it was thought that dispersing them on suitable supports would improve their properties. The supports range from $\gamma\text{-Al}_2\text{O}_3$, which contains considerable amount of basic centers, and SiO_2 , $\text{SiO}_2\text{-Al}_2\text{O}_3$, and Nb_2O_5 , which contain more acid centers. Misono [3, 4], in his review on catalysis by heteropoly acids, quoted that supports containing basic centers bring about the decomposition of the polyanion, and, hence, acidic supports are preferable.

There are conflicting reports on the thermal stability of the supported HPAs, particularly with reference of molybdophosphoric acid supported on Al_2O_3 and $\text{SiO}_2\text{-Al}_2\text{O}_3$ [31]. It is proposed that during the precipitation of the HPAs on supports containing Al_2O_3 , the support interacts with the HPA, forming a compound between

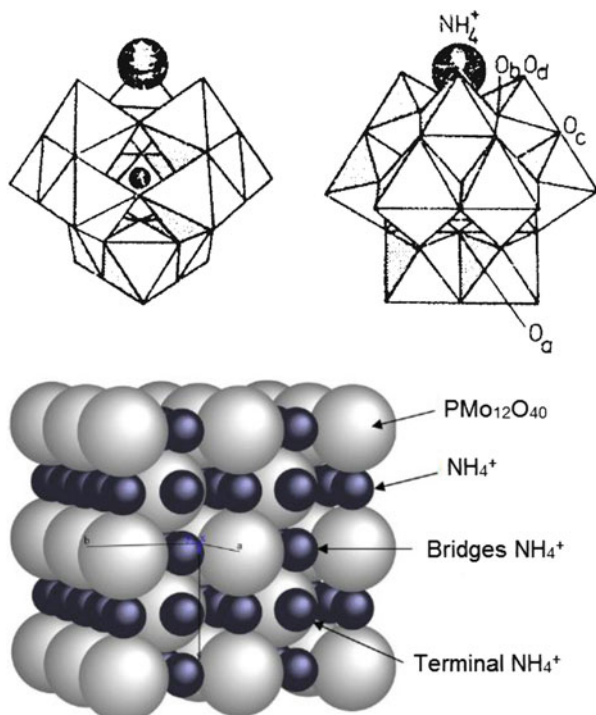


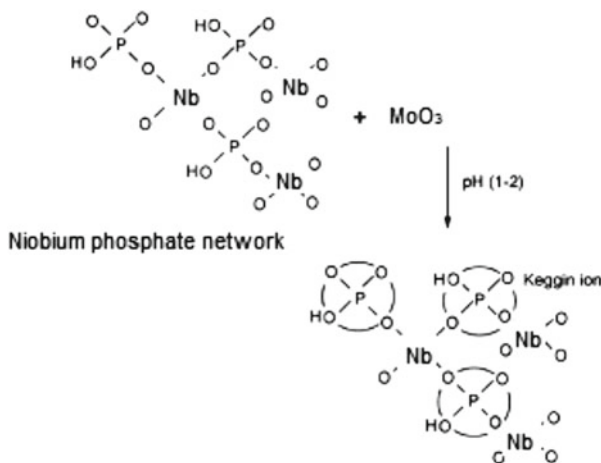
Fig. 2.3 The Keggin unit of AMPA with the position of NH_4^+ ion [30]

the two. In the case of acidic supports, the hydroxyls get protonated and interact with the negative heteropoly ion leading to electrostatic attraction which brings about better dispersion [32]. Better HPA-support interaction improves the thermal stability of the HPA when compared with the bulk acid.

The ammonium salt also contains strong acid sites. The super acidity is reported to be the manifestation of the presence of residual protons in the ammonium salt [33]. Hence, the ammonium salt is also expected to display variation in the nature of HPA-support interaction depending on the acid-base character of the support. Further, the bulk-phase ammonium salt is reported to be thermally more stable than its parent acid.

1.6 In Situ Synthesis of AMPA

The general procedure adopted by Lapham and Moffat [34] and Ito et al. [35] to synthesize ammonium salts of HPAs is a titrimetric method using $(\text{NH}_4)_2\text{CO}_3$, NH_4Cl , NH_4NO_3 , NH_4SO_4 , or $(\text{NH}_4)_2\text{CO}$ solutions and pure heteropoly acid. Ito et al. also described a homogeneous precipitation method to prepare the ammonium salt of HPA. Later, the same groups have studied the effect of temperature and time



Scheme 2.1 Possible route to Keggin ion formation via grafting of MoO_x to the surface of niobium phosphate

of the reaction on the morphology of the acid. As the precipitation temperature increases from 0 to 95 °C, the shape of the ammonium salt aggregate changes from spherical to symmetric decahedral. With the increase in the reaction time from 3 to 24 h, the aggregates are found to be dodecahedral, microporous without mesopore, and highly crystalline. Other methods also exist in the literature for transformation of the hydrogen ions of the parent acid into ammonium ions. Following these methods, one could synthesize the salt with residual protons. In our group, we have synthesized the ammonium salt by using a novel in situ method of preparation (details *vide infra*). The phosphate ions on the support are made to react in situ with the ammonium heptamolybdate in the solution, and, thus, the heteropoly ion is grown at specific sites on the support.

Literature also reveals that ionic interactions between the support surface and HPA clusters help to generate the active species during the impregnation step. However, because of the weak nature of this interaction, it is possible for HPA clusters to leach from the support during reactions in polar solvents. In situ growth of a HPA cluster about a tethered Nb–PO₄ group, such as those found in the framework of a metal phosphate support (Scheme 2.1), could be used to form a bound Keggin-like cluster which may be stable under polar solvents.

Other advantages of in situ process are listed below:

- It avoids usage of corrosion medium like phosphoric acid and the cumbersome ion-exchange procedure.
- The formation of clusters of the salt on the support could be drastically reduced.
- Insolubility of AMPA in common solvents can be obviated in the preparation of supported systems.
- The method can be adapted to various organic and inorganic phosphate precursors.

2 Experimental

2.1 Chemicals and Supports

All solvents and acids used were of A.R. grade (99.9 %). $(\text{NH}_4)_6\text{Mo}_7\text{O}_{24}\cdot 4\text{H}_2\text{O}$, SbCl_3 , and $\text{Bi}(\text{NO}_3)_3\cdot 5\text{H}_2\text{O}$ were supplied by S.D. Fine Chemicals, India. G.R. grade $(\text{NH}_4)_2\text{HPO}_4$, $(\text{NH}_4)_2\text{H}_2\text{PO}_4$, H_3PO_4 and NH_4VO_3 were purchased from Loba Chemie, India. All the supports used were commercial samples TiO_2 -P-25, Degussa, Germany, Nb_2O_5 -AD/1447, CBMM, Brazil, γ - Al_2O_3 -3916R Harshaw, USA, ZrO_2 , Zircon, India, and fluid SiO_2 -53418, AKZO, Japan. These supports were used without further purification. Nb phosphate was supplied by (CBMM, Brazil). 2-methylpyrazine (99 %) was purchased from Aldrich and used without purification.

2.2 Preparation of Various Types of HPA Catalysts

2.2.1 Preparation of AMPA Using Different Phosphorous Precursors

The AMPA catalysts were prepared by dissolving ammonium heptamolybdate [$(\text{NH}_4)_6\text{Mo}_7\text{O}_{24}\cdot 4\text{H}_2\text{O}$] and diammonium hydrogen phosphate (DAHP) $(\text{NH}_4)_2\text{H}(\text{PO}_4)$ in stoichiometric ratio in minimum amount of water. The aqueous solution was first refluxed at 100 °C for 6 h and then concentrated on a water bath to reduce the initial solution to one-third of its volume. The mixture was then slowly heated to get the solid mass, which was dried, first at 120 °C (6 h) and then at 180 °C (6 h). The solid was divided into four equal parts, and each part was subsequently activated at four different temperatures, namely, 400, 450, 500, and 550 °C to get catalysts with different temperatures of activation designated as DAHP catalysts. The same procedure was repeated taking ammonium dihydrogen orthophosphate (ADHP), and the catalysts are designated as ADHP catalysts.

2.2.2 Preparation of Supported AMPA Catalysts

AMPA was first prepared using DAHP, adopting the method described above. The supported catalysts were prepared by impregnating commercial supports, namely, SiO_2 , TiO_2 , ZrO_2 , Al_2O_3 , and Nb_2O_5 with known amounts of aqueous solution of AMPA, followed by drying at 120 °C. All the samples were calcined at 350 °C for 4 h in presence of air. The extent of AMPA loading was thus varied between 5 and 25 wt%.

2.2.3 Preparation of Vanadium Incorporated MPA

Vanadium incorporation into the primary structure of molybdophosphoric acid, i.e., $\text{H}_4\text{PMo}_{11}\text{V}_1\text{O}_{40}$ (MPAV_1) was then taken up. Typically, calculated amount of

disodium hydrogen phosphate was dissolved in water and mixed with required amount of sodium metavanadate that was already dissolved in boiling water. The mixture was cooled and acidified with concentrated sulfuric acid. An aqueous solution of sodium molybdate dihydrate was then added to this mixture. The addition of concentrated sulfuric acid with vigorous stirring resulted in a color change from dark red to light red. The VMPA formed was extracted with diethyl ether as the heteropoly acid was present in middle layer as heteropolyetherate, and the ether was removed by passing through air. The orange solid obtained was dissolved in water and concentrated until the crystals appeared. The prepared catalyst was subsequently calcined in air at 350 °C for 4 h.

In the case of vanadium in the secondary structure of MPA, i.e., $[(VO)_{1.5}PMo_{12}O_{40}]$ (VOMPA), $(VO)^{2+}$ ions were first exchanged with the protons of MPA. Required quantity of V_2O_5 was dissolved in oxalic acid at 100 °C and cooled to room temperature before adding this solution to the aqueous solution of MPA with constant stirring. The excess water was removed on a water bath and the solid sample dried at 120 °C for 12 h. The obtained catalyst was calcined in air at 350 °C for 4 h.

2.2.4 Preparation of Supported Vanadium Incorporated AMPA

The procedure adopted for the preparation of V metal substituted AMPA catalysts was as follows. Ammonium heptamolybdate $[(NH_4)_6Mo_7O_{24} \cdot 6H_2O]$ and diammonium hydrogen orthophosphate $[(NH_4)_2HPO_4]$ were added to water and completely dissolved at a temperature of 80 °C. To this solution, a calculated (depending on the number of V atoms to be incorporated) amount of ammonium metavanadate $[(NH_4)VO_3]$ was added. The contents were refluxed at 100 °C for 6 h, and then dilute HNO_3 was slowly added to the solution to maintain the pH of the solution between 1 and 2. The addition of acid yielded a reddish yellow precipitate. Excess water was then evaporated and the precipitate dried at 120 °C over night and calcined at 350 °C for 4 h in air. The catalyst was designated as vanadium incorporated ammonium salt of 12-molybdophosphoric acid (AMPV).

The supported catalysts were prepared by impregnating commercial supports, namely, SiO_2 , TiO_2 , ZrO_2 , AlF_3 , and CeO_2 , and ceria containing mixed oxides, with known amounts of AMPV salt solution as prepared above followed by drying at 120 °C. All the samples were calcined at 350 °C for 4 h in presence of air. The extent of AMPV loading was also varied between 5 and 25 wt%.

2.2.5 In Situ Synthesis of AMPA

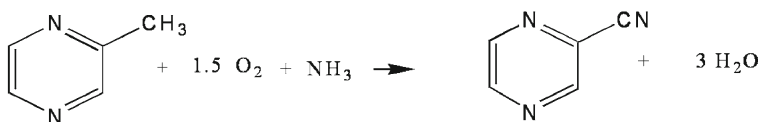
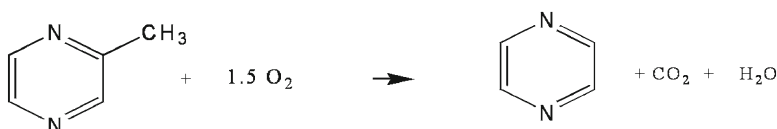
The catalyst was prepared by grafting the polyoxomolybdate species with the phosphate ion of the support. The methodology of preparation was as follows: Catalysts with varying MoO_x loading were prepared by impregnating the metal phosphate supports with known quantities of ammonium heptamolybdate by the wet impregnation method. The amount of Mo in the impregnating solution was selected such that the nominal MoO_3 content varied between 5 and 20 wt%.

The impregnated samples were dried at 120 °C after evaporating the solution in a water bath. The dried masses were then carefully calcined in air at 400 °C over a period of 6 h and kept at that temperature for 4 h.

2.3 Characterization of HPAs

BET surface areas of the catalysts were determined by nitrogen adsorption, at liquid-nitrogen temperature, on a conventional all-glass high-vacuum apparatus. XRD patterns of the catalysts were obtained on a Siemens D-5000 diffractometer using Cu K α radiation. FTIR spectra were recorded on a Biorad-175 C (USA) spectrophotometer following the KBr disc method. Raman spectra were recorded using a Raman microscope (InViaReflex, Renishaw) equipped with deep-depleted thermoelectrically cooled CCD array detector and a high-grade Leica microscope (long working distance objective 20 \times). Raman measurements were made on the sample spot irradiated by a visible 514.5 nm argon ion laser at a fixed laser power of circa 1 mW, exposure time of 10 s, and the spectral resolution of 1–1.3 cm⁻¹ was used. ³¹P MAS NMR spectra of solids were recorded in a 300 MHz Bruker ASX-300 spectrometer. A 4.5 ms pulse (90°) was used with repetition time of 5 s between pulses in order to avoid saturation effects. The spinning rate was 5 kHz. All measurements were carried out at room temperature using 85 % H₃PO₄ as standard reference.

Temperature-programmed reduction (TPR) of the catalysts was carried out in a flow of 10 % H₂/Ar mixture gas at a flow rate of 30 ml/min with a temperature ramp of 10 °C/min. Before the H₂-TPR run, the catalysts were pretreated with Argon gas at 250 °C for 2 h. The hydrogen consumption was monitored using a thermal conductivity detector. TPD of ammonia was carried out on a laboratory built apparatus equipped with a Q-mass detector. In a typical experiment, about 500 mg of oven dried at 110 °C overnight sample was taken in a U-shaped quartz sample tube. Prior to TPDA studies, the catalyst sample was pretreated at 200 °C for 1 h by passing pure helium (99.9 %, 50 ml/min). After pretreatment of the sample, it was saturated with anhydrous ammonia (in a flow of 10 % NH₃-90 % He mixture) at 80 °C with a flow rate of 75 ml/min and was subsequently flushed at 105 °C for 2 h to remove any physisorbed ammonia. Then the TPDA analysis was carried out from ambient temperature to 800 °C at a heating rate of 10 °C/min. The amount of NH₃ evolved (as the sum of ammonia and molecular nitrogen detected) was calculated using GRAMS/32 software. The acidic strength of the solid samples was measured by the potentiometric titration method employing a saturated calomel electrode (SCE). A known mass of solid suspended in acetonitrile was stirred for 3 h, and then the suspension was titrated with a solution of n-butylamine in acetonitrile (0.05N) using a flow rate of 0.05 ml/min. The initial electrode potential (Ei) was assumed to correspond to the maximum acid strength of the surface sites. The acid strength of surface sites was assigned as: very strong sites, Ei > 100 mV; strong sites, 0 < Ei < 100 mV; weak sites, -100 < Ei < 0 mV; and very weak sites, Ei < -100 mV.

1. Ammoxidation:**2. Oxidative Dealkylation:****3. Total Combustion:**

Scheme 2.2 The three possible reactions during ammoxidation of methylpyrazine

2.4 Ammoxidation of MP over HPA Salts

2.4.1 Ammoxidation of 2-Methylpyrazine (MP)

The ammoxidation is basically an oxidation reaction carried out in the presence of ammonia. The reaction is exothermic and is generally carried out in fixed bed reactors at atmospheric pressure. Cyanopyrazine (CP) is the main product of reaction with maximum selectivity approaching 85–100 %. Two other side reactions can also take place; the demethylation of MP gives rise to pyrazine formation, whereas total oxidation leads to formation of carbon dioxide and water vapor. The general scheme for the reaction is described in Scheme 2.2.

2.4.2 Evaluation of Catalysts

The ammoxidation reaction was carried out in a vertical fixed bed, continuous down flow quartz micro-reactor under atmospheric pressure. In a typical experiment, about 3 g of the catalyst (sieved to 18/25 BSS mesh, to avoid mass transfer limitations) diluted with an equal amount of quartz grains was packed between two layers of quartz wool in the reactor. The upper portion of the reactor was filled with quartz beads that served both as a preheater and a mixer for the reactants. Prior to introducing the reactant, MP, the catalyst was treated in ammonia flow at a rate of 20 ml/min for

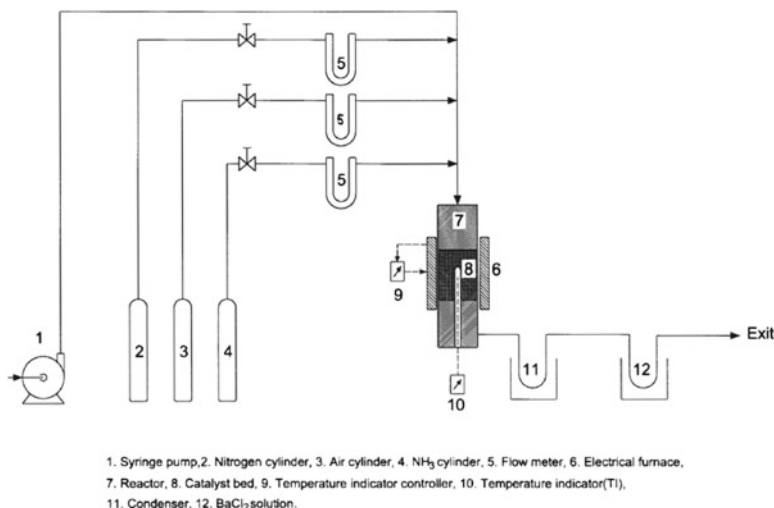


Fig. 2.4 Experimental setup for catalytic activity measurements

1 h. An aqueous mixture of MP (MP: water=1:2.5, v/v) was fed into the reactor by means of a microprocessor-controlled metering pump (B. Braun, Germany). The molar ratio of the feed was kept at MP: water: ammonia: air=1:13:7:38, maintaining a W/F_{liquid} ratio=2.0 g cm⁻³ h. The reaction was studied in the temperature range of 360–420 °C and monitored by a thermocouple with its tip located in the catalyst bed and connected by a PID-type temperature indicator-controller. After allowing the catalyst to attain steady state, at each reaction temperature for 30 min, the product was collected for 15 min and analyzed by gas chromatography, separating it on an OV-101 column (2 m long, 3 mm diameter) using an FID detector. From the analysis of non-condensable exit gas mixture, it was ensured that the quantity of any organic species was negligible. A schematic diagram of the experimental setup is shown in Fig. 2.4.

3 Results and Discussion

3.1 Studies on Bulk MPA and Vanadium Modified MPA (VMPA, VOMPA) Catalysts

Figure 2.5 shows the activity of various MPA catalysts (expressed as percent conversion of MP) during the ammoxidation at different reaction temperatures (360–420 °C). Introduction of vanadium into the Keggin structure (VMPA) is seen influencing the conversion of MP. The activity of the catalyst with vanadium incorporation into the primary structure of MPA (VMPA catalyst) is higher than that of the vanadyl salt (VOMPA) catalyst and pure MPA catalyst. Such a significantly different influence of vanadium atom due to the difference in its location in

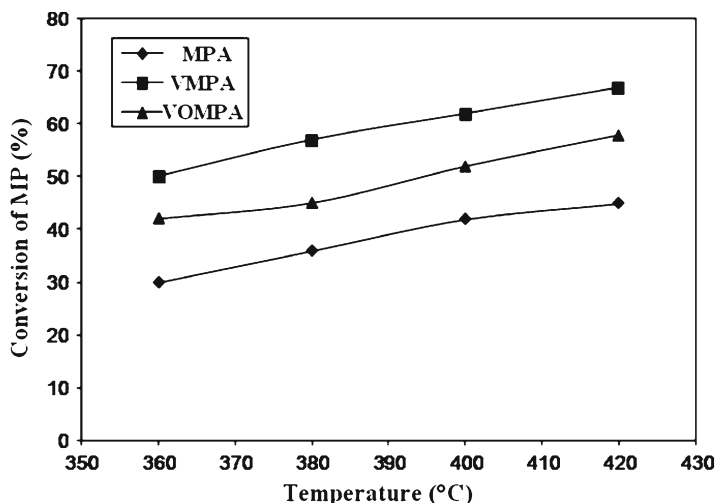


Fig. 2.5 Activity patterns of bulk MPA, VMPA, and VOMPA catalysts at different reaction temperatures (Ref. [36])

heteropoly compound may result in very different susceptibility for reoxidation process. Further evidence to this observation can be obtained by studying the supported catalysts, as stated below.

3.2 Studies on TiO_2 -Supported MPA, VMPA, and VOMPA

The ammoxidation studies conducted on MPA/ TiO_2 , VMPA/ TiO_2 , and VOMPA/ TiO_2 (with 20 wt% active component in the catalysts) expressed in terms of CP yield, at a typical reaction temperature of 380 °C, is shown in Fig. 2.6. The physicochemical properties of the catalysts can be found elsewhere [36]. The catalyst with vanadium incorporation in the primary structure shows higher yield of CP than the vanadium-free MPA catalyst and the catalyst with vanadium in the secondary structure (VOMPA). The difference in the behavior of the catalysts can be attributed to the difference in the location of vanadium atom in the heteropoly acid.

It has been reported that substitution of V^{5+} for Mo^{6+} in MPA results in the generation of more reactive lattice oxygen associated with the Mo–O–V species [37]. The oxidation reaction catalyzed by vanadium occurs by a redox reaction, and it normally follows the Mars–Van Krevelen mechanism. The lattice oxygen helps in the oxidation of the organic substrate, and the gas-phase oxygen supplements the loss of lattice oxygen. The lattice oxygen also plays an important role in the oxidation and reduction cycle of V during the ammoxidation reaction by enhancing its reactivity. The difference in the functionality of vanadium atoms in heteropoly compounds arises due to the very different susceptibility of

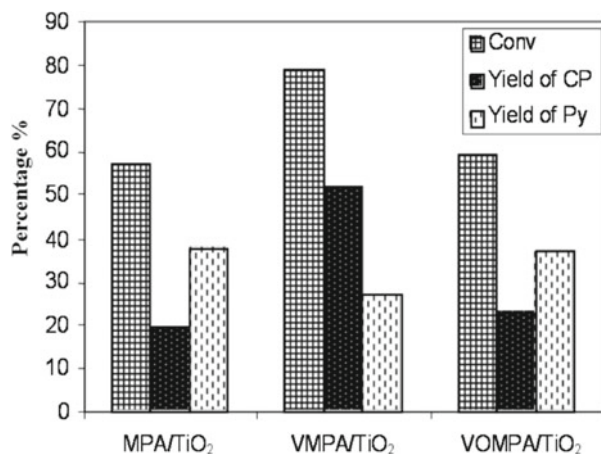
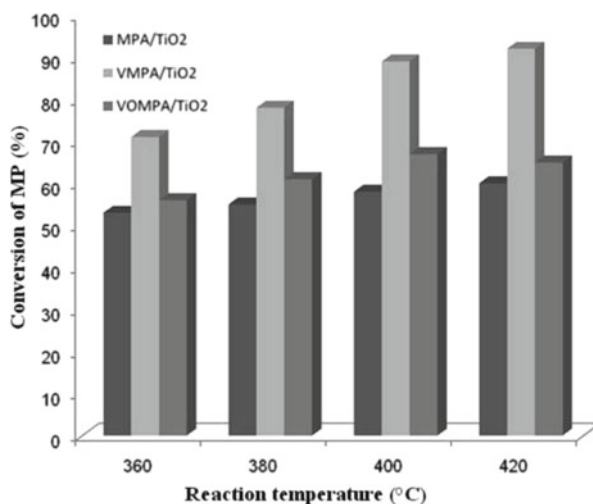


Fig. 2.6 Activity patterns of the TiO₂-supported MPA, VMPA, and VOMPA catalysts at 380 °C (Ref. [36])

Fig. 2.7 Activity patterns of the TiO₂-supported catalysts at various reaction temperatures



vanadyl cations and vanadium atoms in the Keggin structure for reoxidation process [38]. Garte et al. [39] reported that the vanadium atoms present in the Keggin structure, when reduced to V⁴⁺, are easily reoxidized, while the reoxidation of (VO)²⁺ vanadyl ions occurs at a much slower rate even at higher temperature. Thus, it is for this reason that the VMPA/TiO₂ exhibits higher activity than the VOMPA/TiO₂ in the ammoxidation reaction. The effect of reaction temperature is studied over these catalysts and the results are presented in Fig. 2.7. The activity of the catalyst increases with increase in reaction temperature. The activity is found to vary in the following order at any given temperature: VMPA/TiO₂ > VOMPA/TiO₂ > MPA/TiO₂.

3.3 Studies on Bulk AMPA

3.3.1 Comparison of the Structure and Reactivity of the MPA and AMPA Prepared by Precipitation Method

Bondareva et al. [7] have employed a MPA based HPC as catalyst and achieved about 75 % CP yield at lower reaction temperatures (380–390 °C). This catalyst, however, produces 10–25 % byproducts (pyrazine and others) depending on the process conditions. It appears from the open literature that in the ammoxidation reactions attention has been focused on obtaining maximum activity from the catalysts rather than obtaining maximum selectivity, an approach not favorable for development of environmentally acceptable processes. If the molybdenum phosphate based heteropoly acid catalyst can offer maximum selectivity to CP, the process could be acceptable [40]. Bondareva et al. [7] have noticed the formation of AMPA in the used catalysts even though the fresh catalysts were in the acid form. Therefore, it is interesting to observe the functionality of catalysts starting from AMPA itself, since AMPA is also reported to have better thermal stability than MPA [41].

The XRD patterns of the AMPA and MPA, pretreated at different temperatures, in the range 300–500 °C, are shown in Fig. 2.8. The XRD patterns are similar to those reported in our previous publication [42] giving the conclusions: (1) the low-temperature-calcined (300–400 °C) catalysts show the formation of $(\text{NH}_4)_3\text{PMo}_{12}\text{O}_{40}\cdot 4\text{H}_2\text{O}$, agreeing with the data presented by Roch et al. [41] and Albonetti et al. [43], and (2) samples calcined at temperatures 450 °C and above show peaks due to MoO_3 , with the release of ammonia either as such or in the form of nitrogen or its oxides, as also suggested by Damyanova et al. [44] and Hodnett and Moffat [45]. The decomposition of the Keggin ion of AMPA starts at a temperature between 400 and 450 °C, and its complete decomposition occurs at about 500 °C. Peaks due to MoO_3 are observed in the MPA sample calcined at 400 °C as against 450 °C in the case of AMPA. This implies that the structure of the Keggin ion begins to decompose at a temperature between 350 and 400 °C in MPA with partial reduction and distortion of the Keggin unit, as also shown by Tsigdinos [46]. Increase in calcination temperature beyond 450 and 500 °C results in formation of MoO_3 phase. Thus, the thermal stability of MPA is lower compared to AMPA, closely agreeing with what has been reported by McMonagle and Moffat [47].

The FTIR spectra of AMPA and MPA samples subjected to thermal treatment at 300–500 °C are presented at Fig. 2.9. The characteristic peaks due to the Keggin ion, the presence of ammonium ion and a significant shift in the Mo–O_b–Mo band to an extent of 15 cm⁻¹ reveal the formation of AMPA (Fig. 2.9A), as also reported by Deltcheff and Fournier [48]. Calcination at 500 °C has resulted in total disappearance of AMPA and the domination of bands due to MoO_3 . The FTIR spectra of the MPA catalysts calcined at lower temperatures (Fig. 2.9B), i.e., 300–350 °C, show the characteristic bands of the Keggin ion without any distortion. Upon increasing the pretreatment temperature to 400 °C, a broadband in the range of

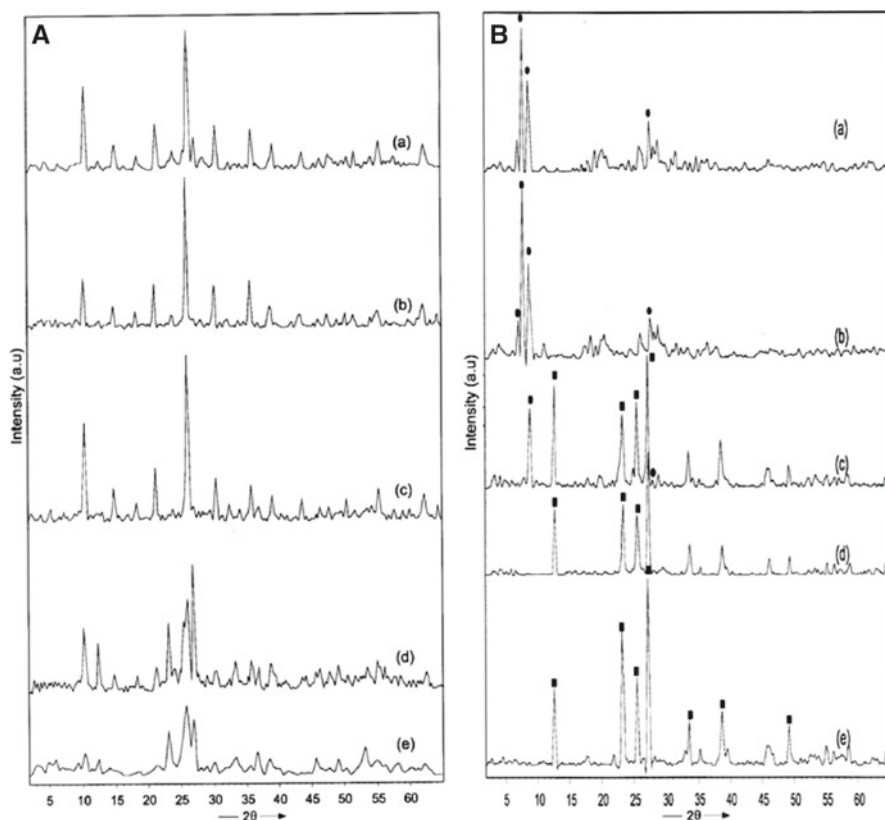


Fig. 2.8 XRD pattern of (A) AMPA and (B) MPA catalysts pretreated at (a) 300 °C, (b) 350 °C, (c) 400 °C, (d) 450 °C, and (e) 500 °C (Ref. [42])

600–1,000 cm^{-1} is observed; this might be due to formation of MoO_3 . The peak at 790 cm^{-1} corresponding to as $(\text{Mo}-\text{O}_c-\text{Mo})$ also becomes very weak, confirming the distortion of the Keggin structure. After calcination at 450–500 °C, the MPA spectra clearly show characteristic bands of MoO_3 , indicating complete destruction of the Keggin ion.

The ^{31}P NMR spectra of AMPA catalysts calcined at different temperatures are shown in Fig. 2.10A. The sample calcined at 300 °C shows two prominent peaks appearing at –5.98 and –12.3 ppm and two more at –5.27 and –7.75 ppm, respectively. The peak at –5.98 ppm corresponds to the $[(\text{NH}_4)_3\text{PMo}_{12}\text{O}_{40}\cdot 4\text{H}_2\text{O}]$ species, and the signals at –5.27 and –7.75 ppm may correspond to dehydrated species and that at –12.3 ppm is for the lacunary species. It is proposed that the signals in the lower field belong to the Keggin ion whether they are dehydrated or the lacunary species. The four different species are similar to those reported by van Veen et al. [49]. These four signals appeared with very little variation in chemical shifts toward upfield after calcination at 350 °C. At 400 °C, the peak at –5.98 ppm becomes very small, and the

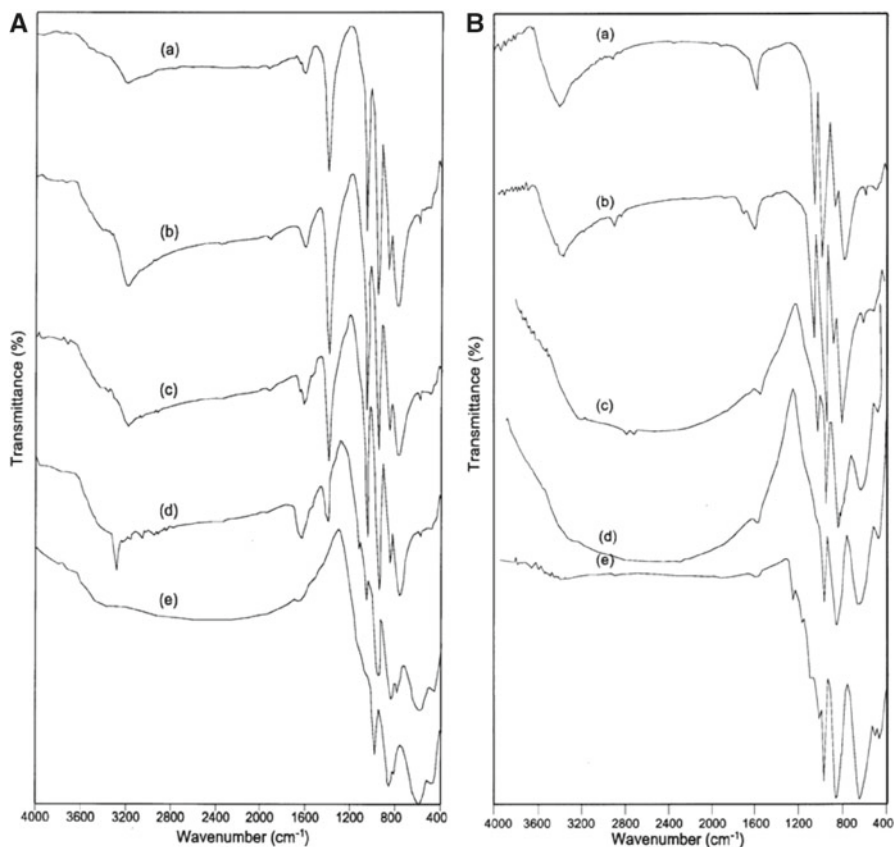


Fig. 2.9 FT-IR spectra of (A) AMPA and (B) MPA catalysts pretreated at (a) 300 °C, (b) 350 °C, (c) 400 °C, (d) 450 °C, and (e) 500 °C (Ref. [42])

peak at -12 ppm vanishes. A new peak appears at 0.56 ppm, which corresponds to monophosphate [50]. This observation clearly reveals the beginning of decomposition of lacunary species into the Mo and P oxides at this temperature. At 450 °C, the two signals at -6.0 and 0.56 ppm can be observed. The peak at 0.56 ppm has shifted to 1.94 ppm due to the decomposition of Keggin ion. At 500 °C, the peaks in the negative side vanish completely with the appearance of only one peak at 1.98 ppm. The peak at 1.94 ppm reflects the formation of P_2O_5 like structure or some unknown molybdenyl phosphate from decomposed Mo and P oxides. These results clearly reveal that the decomposition of Keggin ion completes at this temperature. The signal at 1 ppm appearing in all the samples corresponds to external reference (H_3PO_4).

The ^{31}P NMR spectra of MPA catalysts calcined at different temperatures are shown in Fig. 2.10B. The sample calcined at 300 °C shows two peaks at -1.132 and -2.67 ppm. The former, which is more intense than the latter, corresponds to $[H_3PMo_{12}O_{40} \cdot 9H_2O]$, whereas the latter, which has shifted to up field, corresponds

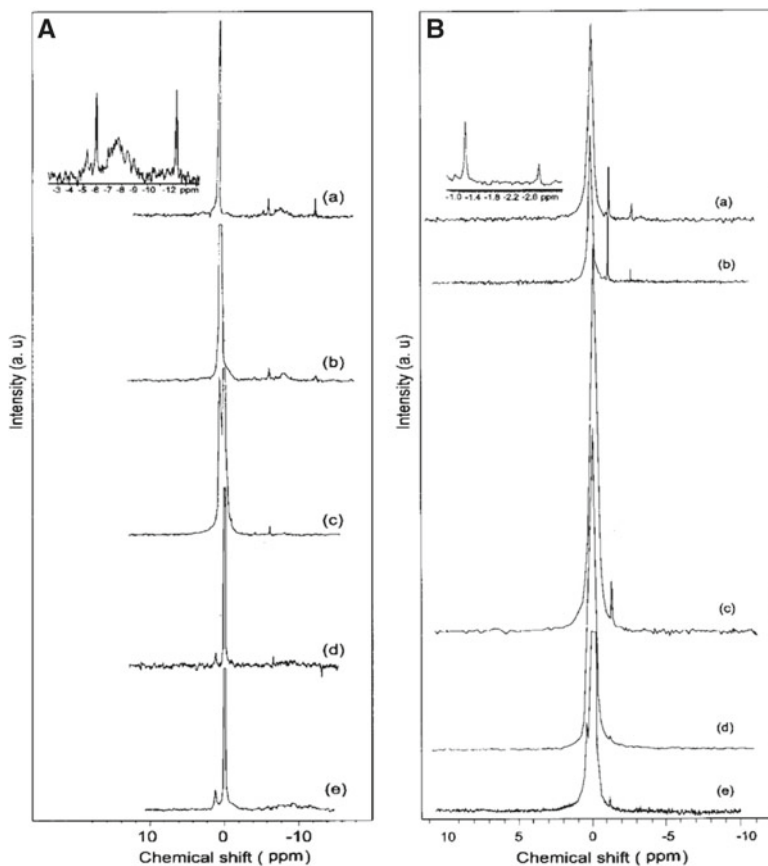


Fig. 2.10 ^{31}P NMR spectra of (A) AMPA and (B) MPA catalysts pretreated at (a) 300 °C, (b) 350 °C, (c) 400 °C, (d) 450 °C, and (e) 500 °C

to dehydrated Keggin ion species [51]. These two signals appear at the same positions in the sample calcined at 350 °C but with decrease in peak intensities. Only one clear peak at -1.15 ppm can be observed in the sample calcined at 400 °C with lesser intensity. The peak at -2.67 ppm disappears. However, a small peak at the positive side, corresponding to monophosphate can be seen.

This change demonstrates the start of the decomposition of Keggin ion at 300 °C. Upon increasing the calcination temperature to 450 °C, the peak which corresponds to Keggin ion becomes very small. A corresponding increase in the signal at 0.42 ppm gives a clear indication that the Keggin ion is almost decomposed to its oxides. The sample calcined at 550 °C shows only peak at 0.42 ppm, indicating complete decomposition. These results are in perfect agreement with the data obtained on XRD and FTIR.

The TPD profiles of AMPA, obtained after various pretreatments, are presented in Fig. 2.11A. The sample calcined at 300 °C exhibits three peaks: one centered

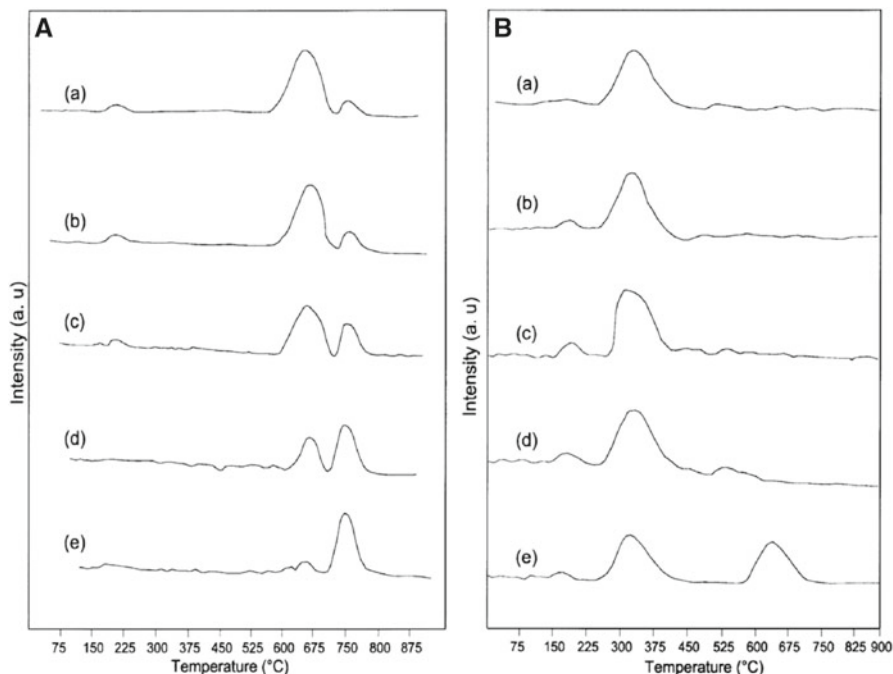


Fig. 2.11 TPDA patterns of (A) AMPA and (B) MPA catalysts pretreated at (a) 300 °C, (b) 350 °C, (c) 400 °C, (d) 450 °C, (e) 500 °C

around 200 °C, a second broad peak centered at 655 °C, and the third desorption peak at 730 °C. Hodnett and Moffat [45] reported that the peak at 200 °C is entirely due to water molecules. Essayem et al. [52] demonstrated two desorption peaks: one due to desorption of NH_3 from the ammonium salt and the other due to desorption of NH_3 from the products formed by the decomposition AMPA at higher temperatures. Upon increasing the pretreatment temperature, the intensity of the peak at 655 °C decreases, and the intensity of the peak at 730 °C increases. As already discussed, the peak due to desorption of NH_3 on the oxides of Mo and P represents the formation thermally decomposed products.

The TPD profiles of MPA pretreated at different temperatures are depicted in Fig. 2.11B. A single desorption peak with its maximum at 360 °C is observed in samples calcined at temperature in the range of 300–400 °C. It is because of desorption of adsorbed ammonia, as reported elsewhere [53]. Ammonia, as a polar molecule, can enter into the whole crystallites and neutralize all the bulk protons resulting in the formation of ammonium salt. Upon increasing the pretreatment temperature to 450–500 °C, a new desorption peak at 655 °C appears, which may correspond to adsorption of NH_3 by the oxides formed during the calcination at higher temperatures. TGA, XRD, FTIR, and ^{31}P NMR results reveal that the decomposition of Keggin ion starts beyond 350 °C in the case of MPA. The samples calcined at 450 and 500 °C have very little capability to adsorb NH_3 molecules because of complete destruction of Keggin structure.

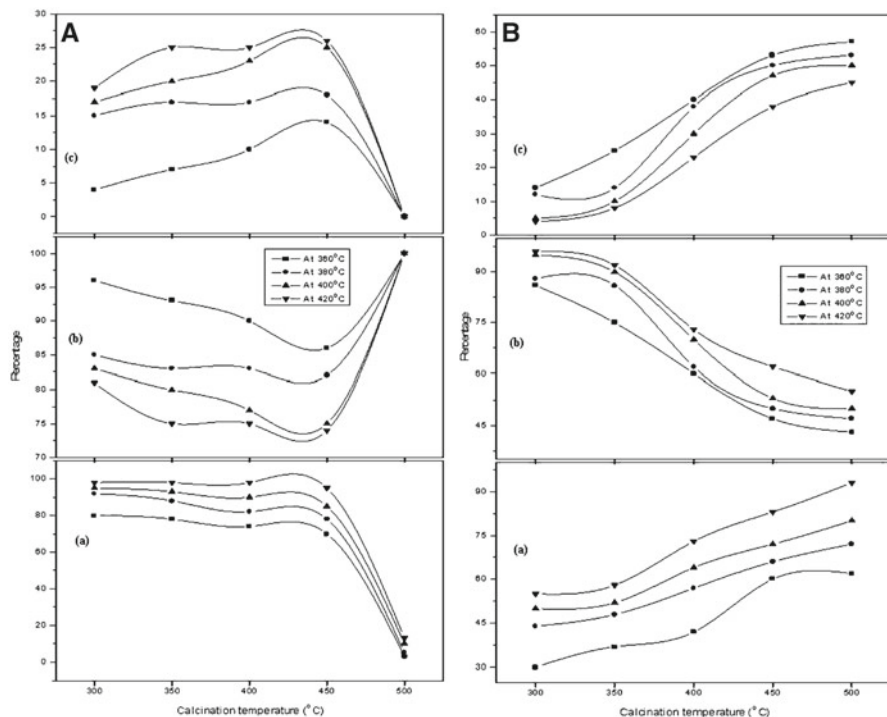
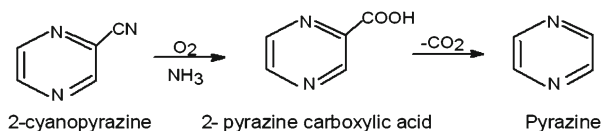


Fig. 2.12 Product distribution of (A) AMPA and (B) MPA catalysts pretreated at different temperatures: (a) conversion of 2-MP, (b) selectivity to CP, (c) selectivity to pyrazine

Variations in activity and selectivity of the catalysts against the temperature of pretreatment as well as reaction temperature are shown in Fig. 2.12A. The AMPA catalysts pretreated in the temperature region 300–450 °C show stable activity reflected in terms of overall conversion at all reaction temperatures in the region of 360–420 °C. Further, the conversion reaches a value of 80 % at the reaction temperature of 360 °C and increases further to a value close to 100 % at 420 °C. Obtaining very high and stable activity is a significant observation. The samples also exhibit very high CP selectivity falling in the region of 75–95 %. Pyrazine levels vary in the range of 5–25 %. Pyrazine formation is reported to be more facile on the acid form of the catalyst. Thus, the tendency to form more pyrazine with increasing calcination temperature can be attributed to the partial decomposition of the ammonium salt leading to the formation of the parent acid. The activity patterns reveal that the AMPA catalyst offers the flexibility of conducting the reaction either at maximum conversion with restricted selectivity or with high selectivity at restricted conversion, the latter being environmentally highly attractive.

The activity dropped to very low value when the pretreatment temperature reaches 500 °C. From the XRD, FTIR, ^{31}P NMR, and TPDA results, it can be understood that the catalyst retains the structure of AMPA up to 450 °C, beyond which there is complete destruction of Keggin unit with the release of ammonia and the formation of

Scheme 2.3 Possible reaction pathways of pyrazine formation from cyanopyrazine



oxides of molybdenum and phosphorous. Thus, it may be expected that as long as the catalyst exists in the form of AMPA, higher activity can be realized. The partially decomposed salt can be regenerated during the reaction. Albonetti et al. [43] also have observed ammonium salt to be more reactive than the acid itself in the formation of methacrylic acid from isobutyric acid. The effect of the cation is related either to its electronegativity affecting the Mo oxidation state or to the modification of acidity.

Increase in reaction temperature from 360 to 420 °C is seen to increase the MP conversion, as a consequence of increase in reaction rate. However, the selectivity toward CP decreases and that of pyrazine increases. Partial dehydration of the catalyst and formation of the acid from the compound could be attributed to the increase in selectivity to pyrazine. Bondareva et al. [7] has also observed increase in pyrazine selectivity at higher reaction temperatures. They are of the opinion that as the MP conversion exceeds 80 %, the oxidation of CP occurs leading to pyrazine production. The reaction pattern is shown below in Scheme 2.3.

The product distribution in the ammoxidation reaction over MPA catalysts is shown in Fig. 2.12B. The conversion level gradually increases from 30 to 90 % when the pretreatment temperature is increased from 300 to 500 °C. Even though the MPA catalyst exhibits a facile decomposition at lower temperatures compared to that of AMPA, the increase in conversion with increase in calcination temperature can be attributed to the transformation of the oxides into the AMPA structure during the reaction, as also revealed by the XRD patterns of the used catalysts. This seems to be the main reason for higher conversion levels of the MPA catalysts pretreated at higher temperatures. The selectivity to CP, however, is decreasing with increase in pretreatment temperature. It is clear that the presence of AMPA is advantageous to get higher selectivity to CP. The samples calcined at lower temperatures have preserved the Keggin ion structure. The transformation of MPA into AMPA could be more facile during the reaction than the transformation of the oxides obtained at higher calcination temperatures. The transformation in the latter case may not be complete as revealed by the XRD of the used samples. Very high pyrazine selectivity exhibited by the MPA samples calcined at high temperatures also suggest that the AMPA form of the catalyst is much better both economically and environmentally.

3.3.2 Influence of Phosphate Precursor on Ammoxidation Activity

Preparation of AMPA by precipitation method, at controlled pH, using DAHP as the precursor is observed to be the best method than using ADHP in terms of obtaining relatively pure form of AMPA. The ^{31}P NMR spectra of the two catalysts (DAHP and ADHP) are shown in Fig. 2.13A, B. The DAHP sample calcined at 400 °C shows

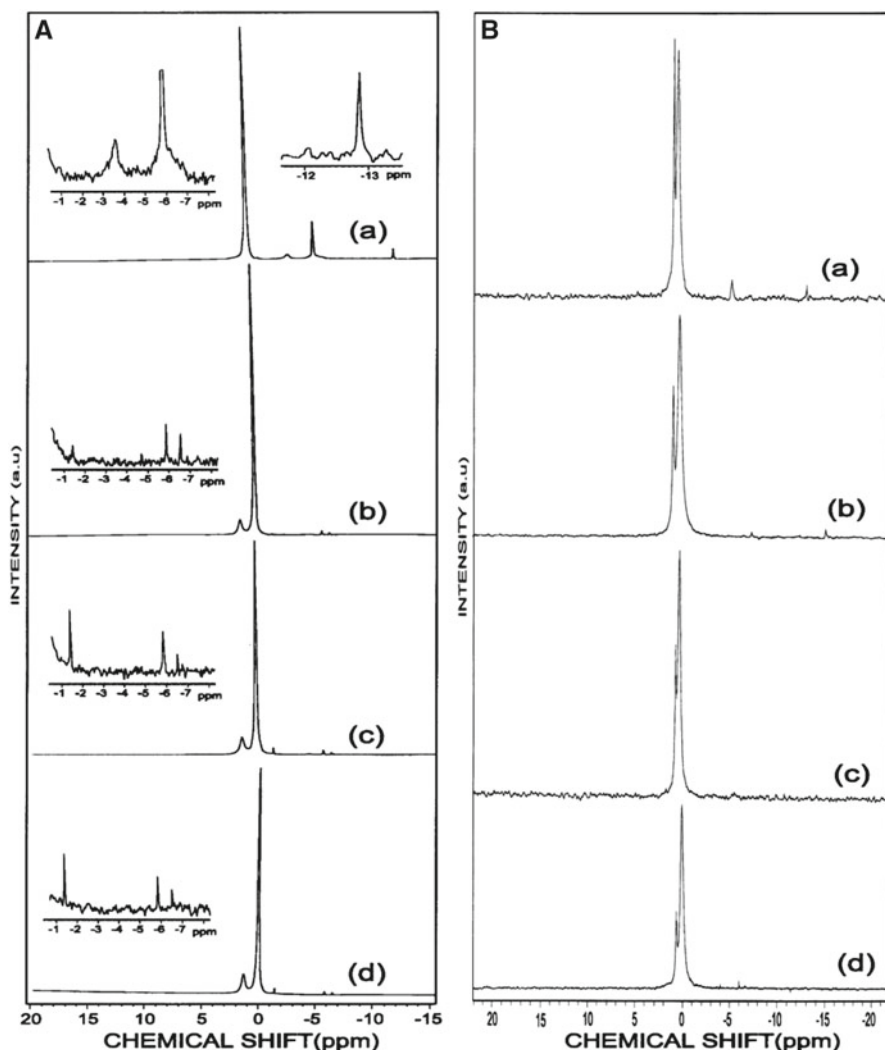
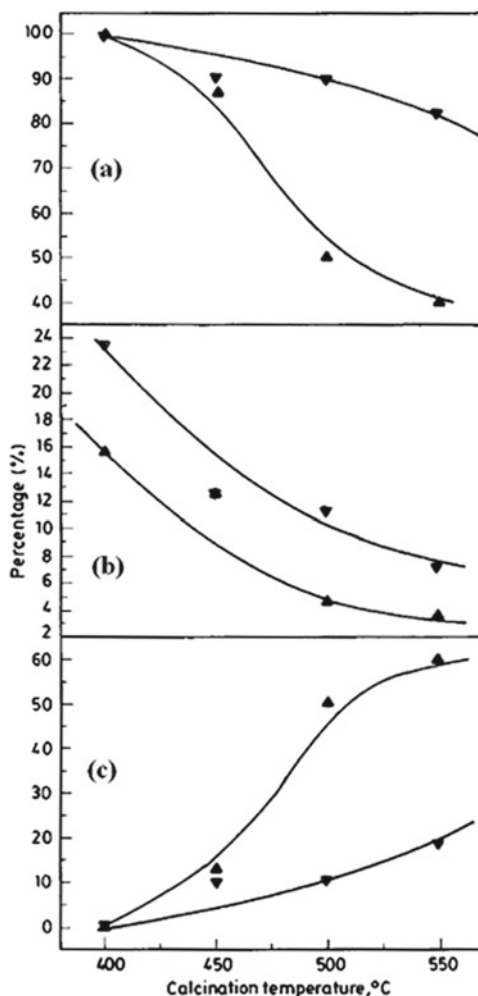


Fig. 2.13 ^{31}P NMR spectra of (A) DAHP catalysts and (B) ADHP catalysts at different calcination temperatures: (a) 400 °C, (b) 450 °C, (c) 500 °C, and (d) 550 °C (Unpublished data or PhD thesis of K.N. Rao, Jawaharlal Nehru Technological University, India 2004)

peaks at -3.5 and -5.8 ppm corresponding to Keggin ion $[\text{PMo}_{12}\text{O}_{40}]^{3-}$ and the dehydrated Keggin ion $[\text{PMo}_{12}\text{O}_{38}]^{3-}$ species [54]. The low-intensity peak seen at -13.0 ppm may be attributed to decomposed Keggin species [50]. The catalyst sample calcined at 450 °C shows reduction in the intensity of -3.5 and -6.0 ppm peaks (clearly shown in inset of the Fig. 2.13A). A new peak is observed at 1.4 ppm, which may be due to the basic molybdenum phosphate [55]. As the calcination temperature increases to 500 and 550 °C, the intensity of -6.0 ppm peak reduces very much and that of the 1.4 ppm

Fig. 2.14 Influence of calcination temperature on ammoxidation functionalities of catalysts at a reaction temperature of 380 °C:
 (a) selectivity to CP,
 (b) conversion of MP, and
 (c) selectivity to pyrazine
 (▲) DAHP and (▼) ADHP catalysts



peak increases presumably because of formation of stable basic molybdenum phosphate. The ADHP catalyst sample calcined at 400 °C shows a small peak at −4.0 ppm corresponding to Keggin ion along with a major peak at 0.56 ppm, which may be due to free phosphate or P_2O_5 like structure [50]. With increase in calcination temperature, the intensity of 0.56 ppm peak increases revealing the complete conversion of reactants to unknown compounds. The ^{31}P NMR results clearly corroborate the conclusions drawn from XRD and FTIR results (not shown).

The AMPA and not MPA as such, is found to be responsible for the activity and selectivity of the catalysts used in MP ammoxidation. This observation is confirmed by correlating the ammonium content of the catalyst with its activity during the ammoxidation. Optimization of the quantity of ammonium salt in the catalyst has resulted in identification of the maximum selectivity toward CP (Fig. 2.14).

Table 2.1 BET surface area and acidic strength values of the various heteropoly acid catalysts

Catalyst	BET surface area (m ² /g)	Acidic strength (Ei, mV)
NbPO ₄	146	378
AMPA-NbPO ₄ -5 ^a	85	530
AMPA-NbPO ₄ -10 ^a	79	543
AMPA-NbPO ₄ -15 ^a	41	581
AMPA-NbPO ₄ -20 ^a	34	560
FePO ₄	2.3	333
AMPA-FePO ₄ -5 ^a	3.1	368
AMPA-FePO ₄ -10 ^a	12	469
AMPA-FePO ₄ -15 ^a	6.5	528
AMPA-FePO ₄ -20 ^a	5.1	564
α-VOPO ₄	2.2	798
β-VOPO ₄	1.4	528
AMPA-α-VOPO ₄	6.6	825
AMPA-β-VOPO ₄	2.8	586
		Ammonia evolved by TPD (mmol/g)
DAHP-400 ^b	4.5	5.04 × 10 ⁻²
DAHP-450 ^b	3.5	3.88 × 10 ⁻²
DAHP-500 ^b	2.0	3.00 × 10 ⁻²
DAHP-550 ^b	1.0	1.85 × 10 ⁻²
ADHP-400 ^b	3.4	4.40 × 10 ⁻²
ADHP-450 ^b	2.1	1.44 × 10 ⁻²
ADHP-500 ^b	1.6	1.12 × 10 ⁻²
ADHP-550 ^b	0.8	9.32 × 10 ⁻³

^aMo-loading (wt%)^bCalcination temperature

Formation of AMPA is more favorable when the reactant salt contains more ammonia in the precursor salt, as in the case of catalysts prepared using diammonium hydrogen orthophosphate (Table 2.1). Formation of thermally stable basic molybdenum phosphate at high calcination temperatures and its facile transformation to AMPA during the reaction make it a better active and selective ammoxidation catalyst, compared to the less ammonia containing catalyst prepared by using ammonium dihydrogen orthophosphate.

3.4 Studies on AMPA Supported on Nb₂O₅, SiO₂, TiO₂, ZrO₂, and Al₂O₃

Even though it is proved that using AMPA in place of MPA is beneficial for getting enhanced activity and selectivity during ammoxidation of MP, there have been no detailed studies on the supported AMPA catalysts. Giving due consideration for this observation, it is found to be prudent to carry out a systematic study on AMPA

Table 2.2 BET surface area and acidic strength values of different supports and 20 % AMPA-supported catalysts

S. no.	Catalyst	BET surface area (m ² /g)	Amount of ammonia desorbed (mmol/g)
1	Hydrated Nb ₂ O ₅	140	2.12×10^{-1}
2	SiO ₂	300	1.96×10^{-1}
3	TiO ₂	55	4.58×10^{-2}
4	ZrO ₂	20	0.98×10^{-1}
5	Al ₂ O ₃	196	1.10×10^{-1}
6	20 %AMPA/HNb ₂ O ₅	43	6.92×10^{-2}
7	20 %AMPA/SiO ₂	184	3.96×10^{-1}
8	20 %AMPA/TiO ₂	1.4	5.57×10^{-2}
9	20 %AMPA/ZrO ₂	2	8.54×10^{-2}
10	20 %AMPA/Al ₂ O ₃	119	4.93×10^{-2}

supported on different supports like Nb₂O₅, SiO₂, TiO₂, ZrO₂, and Al₂O₃. The surface area, acidity, and nature of the support play an important role in ammoxidation to obtain high activity and selectivity. The BET surface area and acidity values of different supports and 20 % AMPA-supported catalysts are presented in Table 2.2. It is known that supports, which contain basic centers, bring about the decomposition of the polyanion, due to the interaction of the HPA with the support forming a compound between the two. In the case of acidic supports, the hydroxyls get protonated and interact with the negative heteropoly ion leading to electrostatic attraction which brings about better dispersion. Better HPA-support interaction improves the thermal stability of the HPA when compared with the bulk acid. The ammonium salt also contains strong acid sites. The super acidity is reported to be the manifestation of the presence of residual protons in the ammonium salt [33]. However, the ammonium salt is also expected to display variation in the nature of HPA-support interaction depending on the acid-base characteristics of the support.

XRD, FTIR, and ³¹P NMR studies on AMPA/TiO₂ catalysts have shown (Figs. 2.15 and 2.16) that AMPA is well dispersed until 15 wt% loading due to strong electrostatic interaction between complex Keggin [PMo₁₂O₄₀]³⁻ ion with the positively charged hydroxyls on the TiO₂ support. At higher loadings, the formation of crystalline AMPA [(NH₄)₃PO₄(MoO₃)₁₂·4H₂O)] indicating the completion of interaction at 15 wt% is seen. The temperature-programmed desorption of ammonia studies (Fig. 2.17) on AMPA/TiO₂ catalysts reveal that with increase of AMPA loading there is a decrease in Lewis acidity and increase in Bronsted acidity of the supported catalysts. The increase in Bronsted acidity is associated with bulk AMPA formation. More details can be found in our previous publications [56, 57].

A comparison of ammoxidation activity obtained at 20 wt% AMPA supported on Nb₂O₅, SiO₂, TiO₂, ZrO₂, and Al₂O₃ obtained at 380 °C is shown in Fig. 2.18. The activity and selectivity obtained on the catalysts are in the following order: AMPA/Nb₂O₅ > AMPA/ZrO₂ > AMPA/TiO₂ > AMPA/SiO₂ > AMPA/Al₂O₃.

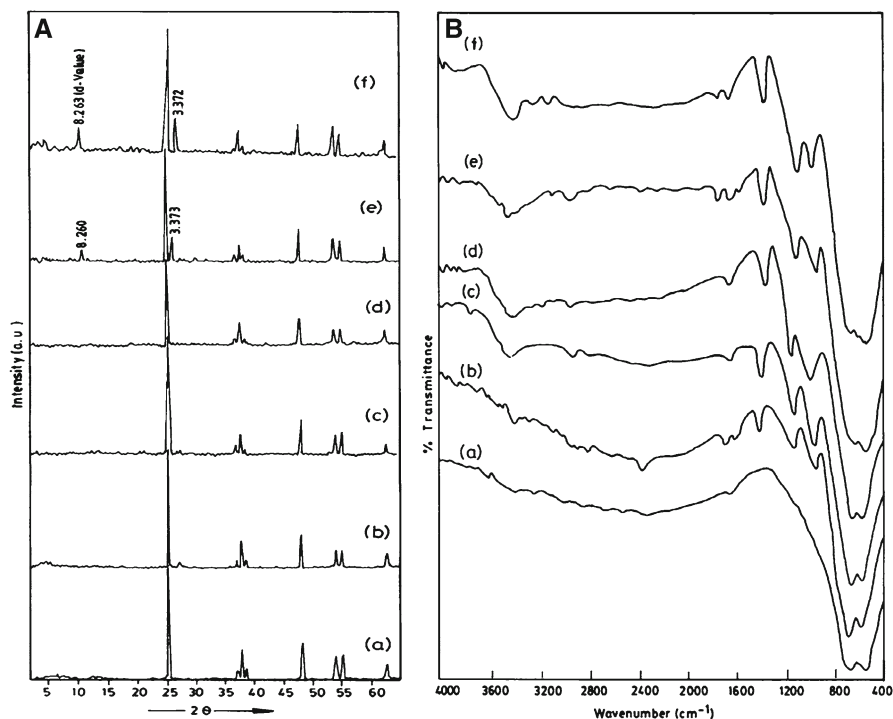


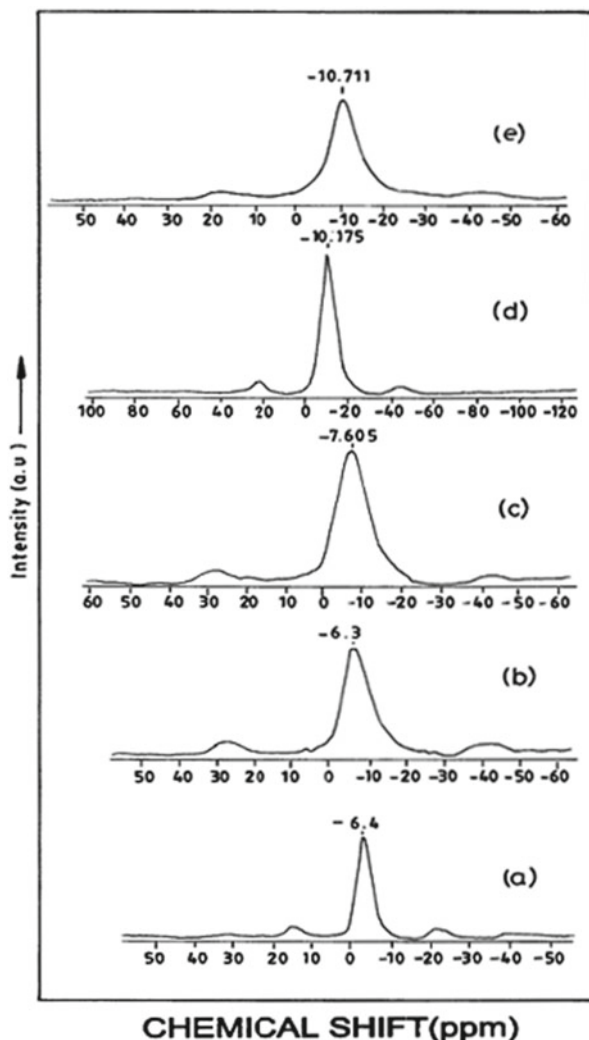
Fig. 2.15 (A) XRD and (B) FTIR patterns of TiO_2 -supported AMPA catalysts: (a) support (b) AMPA-5, (c) AMPA-10, (d) AMPA-15, (e) AMPA- 20, (f) AMPA-25 (Ref. [56])

Nb_2O_5 - and ZrO_2 -supported catalysts show higher activity and selectivity because of high Bronsted acidity of AMPA, whereas silica-supported AMPA catalyst contains highest acidity than the other catalysts and hence shown very less selectivity toward CP because of its Lewis acidity generated by interaction of surface hydroxyl groups of silica with AMPA.

3.4.1 Half-Bandwidth Analysis: A Novel Method to Determine the Dispersion of HPA-Supported Catalysts [56]

The chemical interactions between the HPCs and the support are a matter of great interest because a strong interaction could fix the HPC to the carrier, avoiding the leaching of heteropoly compound in the reaction media or maintaining its high dispersion [32]. The determination of dispersion of active phase on the support is important to understand the role of active phase in reaction mechanism. It is not possible to determine the dispersion of HPC on the support by using conventional gas adsorption measurements. A novel approach called IR half-bandwidth analysis has been developed by our group to determine the dispersion of HPCs. By taking

Fig. 2.16 ^{31}P NMR spectra of TiO_2 -supported AMPA catalysts: (a) AMPA-5, (b) AMPA-10, (c) AMPA-15, (d) AMPA-20, and (e) AMPA-25 (Ref. [56])



the $\text{P}=\text{O}$ band at $1,060\text{ cm}^{-1}$ as reference, the half-bandwidth was measured for different AMPA loaded catalysts. The half-bandwidth of the catalysts increases linearly from 5 to 15 wt% AMPA loading, and beyond 15 wt%, it is almost equal for higher-loaded catalysts (Fig. 2.19). This indicates that the monolayer saturation occurs between 10 and 15 wt%. Above 15 wt% loading, the catalysts acquire bulk nature by forming multi-layers of AMPA.

A correlation between the half-bandwidth and ammoxidation functionality is shown in Fig. 2.19. The values of MP conversion on bulk AMPA are 5 and 23 % at 360 and 380 °C, respectively. The conversion has increased up to 15 wt% loading

Fig. 2.17 TPDA spectra of TiO_2 -supported AMPA catalysts: (a) support, (b) AMPA-5 (c) AMPA-10, (d) AMPA-15, (e) AMPA-20, (f) AMPA-25

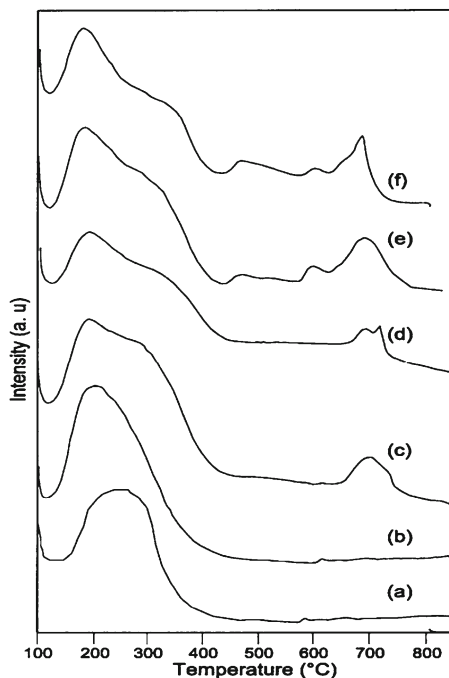
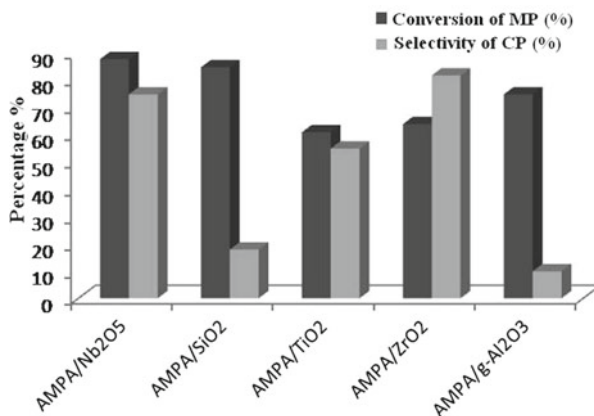


Fig. 2.18 Ammoxidation activity profiles of the supported AMPA (20 wt%) catalysts at 380 °C



and thereafter remains almost constant. The values of the half-width of the $1,060\text{ cm}^{-1}$ band also have displayed a similar trend. Hence, it appears that the extent of interaction of the salt with the support reaches a maximum at about 15 wt%. Further increase in loading (where crystallization of the salt is observed) does not increase the conversion. This observation may be valuable in the characterization of supported HPAs and their salts in determining the maximum extent of loading where the activity is also the maximum.

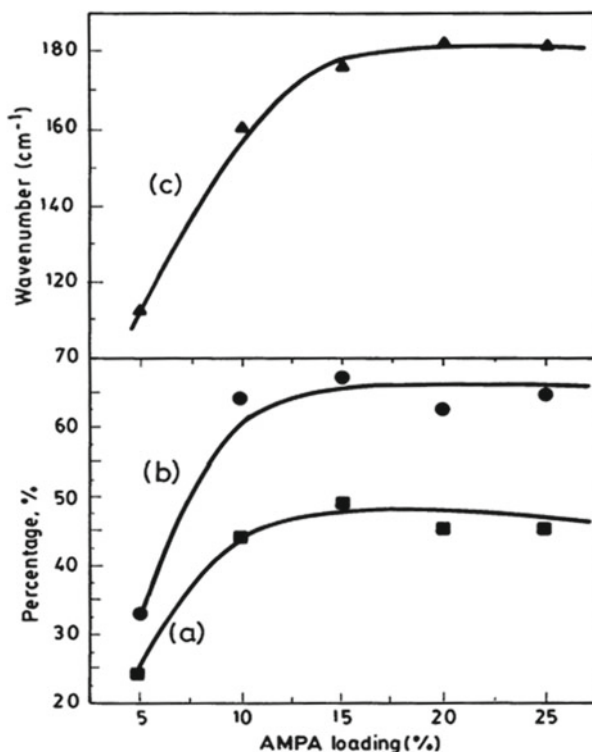


Fig. 2.19 Correlation between half-bandwidth and ammoxidation activity of the TiO_2 -supported AMPA catalysts (a) conversion of MP at 360°C , (b) conversion of MP at 380°C , and (c) half-bandwidth of $1,060\text{ cm}^{-1}$ band (Ref. [56])

3.5 In Situ Synthesized AMPA-Based Systems

3.5.1 AMPA/ NbOPO_4 Catalysts

It is interesting to verify whether in situ synthesis of AMPA on various supports is possible, so we have used NbOPO_4 , VOPO_4 , and FePO_4 to prepare AMPA by in situ technique, which markedly enhances the ammoxidation activity. The enhancement in the activity as correlated with the extent of salt formation has been discussed in our previous publications [58–62]. Figure 2.20A shows the XRD patterns of the AMPA generated using niobium phosphate as the support, as a function of MoO_3 content for the catalysts along with that of pure niobium phosphate. The formation of AMPA with the formula $(\text{NH}_4)_3\text{PO}_4(\text{MoO}_3)_{12}\cdot 4\text{H}_2\text{O}$ (ASTM Card No-09-412) can be clearly observed in all the catalysts from 5 to 20 wt% of MoO_3 . The present observation is very significant in the sense that the formation of AMPA exhibiting the Keggin structure occurs by participation of the surface phosphate of the support, contrary to the general methods of preparation of AMPA, wherein the phosphate

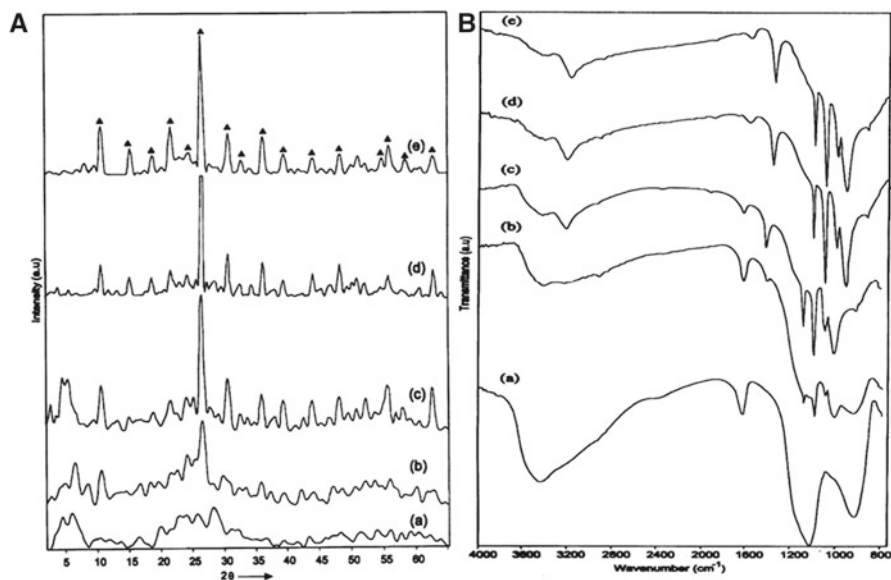
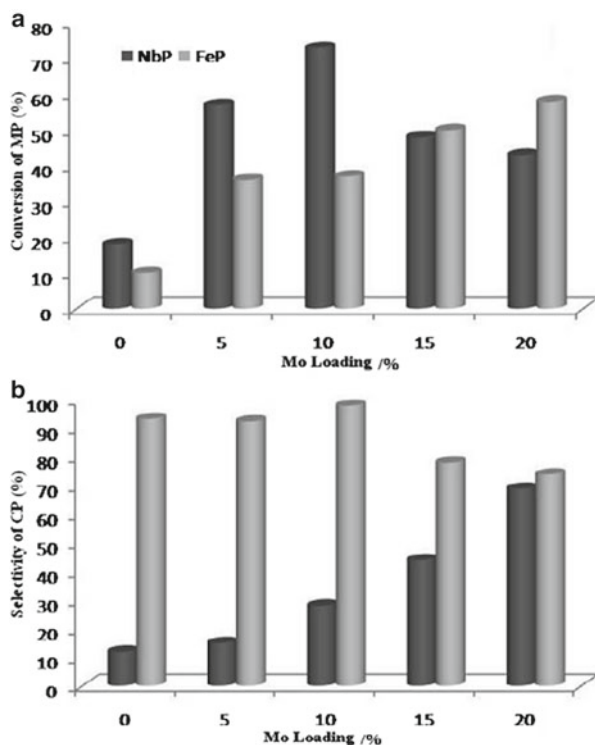


Fig. 2.20 (A) XRD and (B) FTIR spectra of AMPA-NbPO₄ catalysts: (a) NbPO₄, (b) AMPA-5, (c) AMPA-10, (d) AMPA-15, and (e) AMPA-20 (Ref. [58])

species are added in the form of phosphoric acid or its ammonium salts along with the Mo salt. Since powder X-ray diffraction patterns have not evidenced any discrete molybdenum containing phases, further characterization studies of AMPA/NbOPO₄ catalysts have been carried out by FTIR spectroscopy. FTIR spectra of catalysts prior to reaction are given in Fig. 2.20B. On the basis of previous literature, the features at 1,064, 970, and 870 cm⁻¹ which are present in all the four catalysts have been assigned to Keggin structure in the moiety. Increase in the intensity of these bands with the AMPA content in the catalyst can be observed. In order to confirm whether the formation of AMPA is confined to the surface of the niobium phosphate or niobium enters into the primary structure of Keggin unit, a comparison of the positions of the bands with those reported in the literature is made. As there is no noticeable shift in the bands, it is considered that the formation of AMPA is confined to the surface of the niobium phosphate support, and niobium is not incorporated into the primary structure of the Keggin unit. FTIR studies on the catalysts correlate with the XRD results and do not show any formation of molybdenum trioxide species in the catalysts. Pronounced dependence of ammoxidation activity upon AMPA loading shown in Fig. 2.21 is due to increase in formation of highly dispersed AMPA content in the catalysts (5–10 wt% AMPA/NbOPO₄), whereas the decrease in activity in 15–20 wt% is due to formation of bulk crystallites of AMPA which resist diffusion of reactant species by blocking the pores. Details of the activity studies conducted at various temperatures can be found elsewhere [58]. The selectivity toward cyanopyrazine obtained a maximum value of 69 % on 20 wt% AMPA/NbOPO₄ at 380 °C.

Fig. 2.21 Comparison of activity for ammoxidation of MP for AMPA-NbPO₄ and AMPA-FePO₄ catalysts: (a) conversion of MP, (b) selectivity to CP at 380 °C



3.5.2 Studies on AMPA/FePO₄ Catalysts

In order to design a highly selective catalyst for MP ammoxidation, attention has been paid on iron phosphate [59]. Iron phosphate is found to be less active and highly selective and shows 98 % CP selectivity compared to AMPA/NbOPO₄. The AMPA/FePO₄ catalysts have also showed enhancement in the activity while retaining the CP selectivity of iron phosphate to a large extent as seen in Fig. 2.21. The high selectivity of iron phosphate can be explained as due to the absence of labile M=O bonds which otherwise contributes to oxygen insertion. It could also be due to the ease of formation of an ammonium complex of the type NH₄FeP₂O₇. Formation of Mo oxide phase is observed at higher loadings of ≥15 wt% in the XRD spectra. This observation is further supported by FTIR and Raman spectroscopy [60] analysis. The formation of Mo oxide could be the reason for the decline in selectivity at higher loadings.

3.5.3 Studies on AMPA/VOPO₄ Catalysts

Two VOPO₄ (α- and β) and two 20 wt% AMPA-VOPO₄ (α- and β) catalysts are selected and tested for their activity in ammoxidation. The influence of reaction temperature on the conversion of MP is shown in Fig. 2.22. Phase composition is

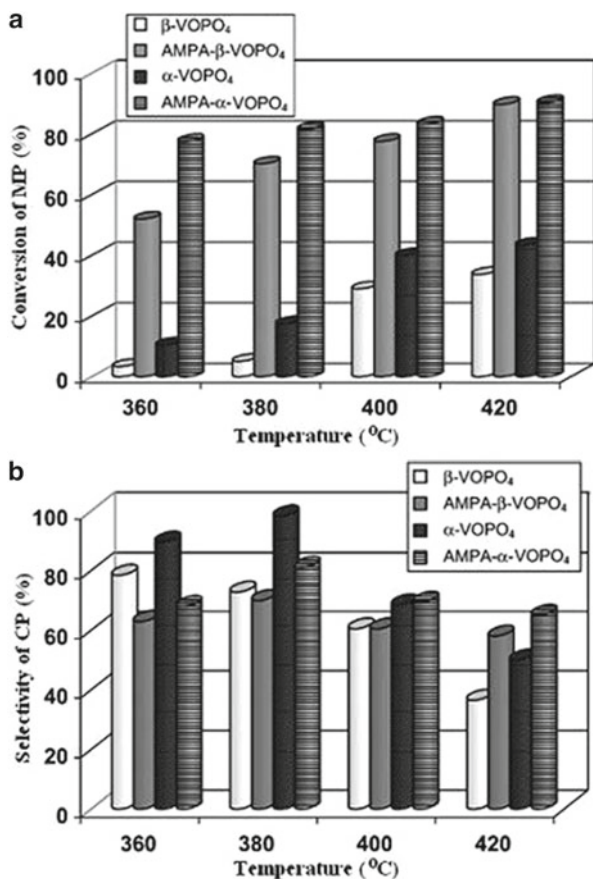
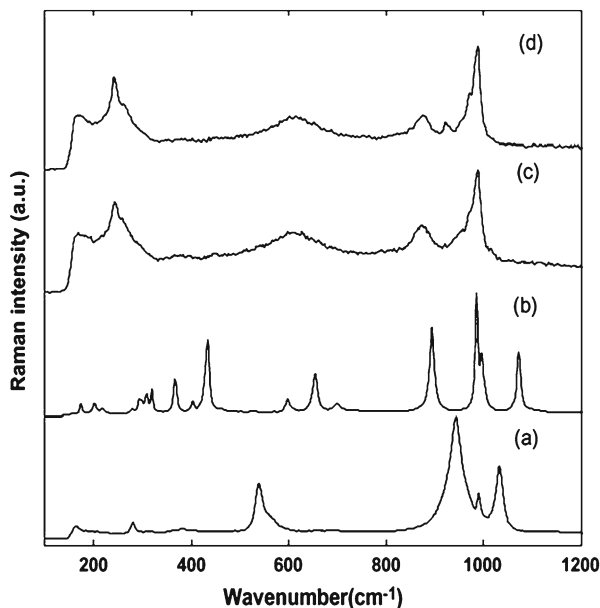


Fig. 2.22 (a) Influence of reaction temperature on the catalytic performance of VOPO₄ and AMPA-VOPO₄ catalysts. (b) Variation of CP selectivity as a function of reaction temperature over VOPO₄ and AMPA-VOPO₄ catalysts (Ref. [61])

identified by Raman spectroscopy and the data are shown in Fig. 2.23. Detailed description of all the spectra can be found elsewhere [61, 62]. The main characteristic features of the Keggin structure in the spectra c and d can be observed at 988 cm⁻¹ (ν s Mo–Od), 919–877 cm⁻¹ (ν as Mo–O_b–Mo), and 598–615 cm⁻¹ (ν as Mo–O_c–Mo) with an important bridge stretching character. The spectra agree well with those values reported in the literature [63]. Thus, the information obtained from the Raman data confirms the formation of AMPA on the VOPO₄ materials. Figure 2.22 clearly demonstrates that the reaction temperature has a promotional effect on the conversion of MP irrespective of the nature of catalyst applied. It is also obvious that there is a distinct influence of in situ synthesized AMPA samples on the catalytic performance compared to their corresponding analogues. Both α - and β -VOPO₄ compose of AMPA exhibited better performance in comparison with their parent α - and β -VOPO₄ samples. Another interesting observation is that between these AMPA-containing solids, the α -form of AMPA displayed better performance compared to its

Fig. 2.23 Raman spectra of catalysts: (a) α -VOPO₄, (b) β -VOPO₄, (c) AMPA- α -VOPO₄, (d) AMPA- β -VOPO₄ (Ref. [61])



β -form. In a similar way, between the two monophosphates tested, the α -VOPO₄ is observed to show somewhat higher activity than β -VOPO₄. It is reasonable to assume that the differences in the activity of these two monophosphates could be due to the differences in the structures of these VOPO₄ solids, i.e., α -VOPO₄ consisting of a layered structure, whereas β -VOPO₄ showing a three-dimensional one.

The acidity characteristics of the catalysts are another possible reason for such deviations in their catalytic performance. For instance, the highly acidic samples of this study such as AMPA- α -VOPO₄ and α -VOPO₄ (see Table 2.1) exhibit higher activity and selectivity and thus lend support to the above assumption that acidity plays a critical role on the catalytic performance. It can be deduced that the presence of AMPA enhances the Brønsted acidity of the catalysts. Such enhancement in the Brønsted acidity in turn increases the ammonia adsorption capacity of the catalysts. This seems to be the more probable reason for the increased activity of the AMPA/ α -VOPO₄ catalysts. As shown in the Fig. 2.22, temperature has profound influence on the selectivity of CP, α -VOPO₄ exhibiting the highest selectivity $\geq 95\%$ but only a low degree of conversion $\leq 5\%$. However, with rise in conversion levels, the CP selectivity is significantly decreased. The AMPA catalysts disclose a slightly lower selectivity (60–70 %) but remarkably higher conversions (55–90 %) than the pure VOPO₄ catalysts (CP selectivity = 60–95 % and conversion of MP = 5–30 %). Overall, better yields have been obtained over in situ synthesized AMPA-containing VOPO₄ solids compared to their corresponding analogues.

XRD and the FTIR data obtained on the spent samples [62] reveal that the VOPO₄ catalysts partly transformed into the ammonium-containing vanadium phosphates,

Table 2.3 Phase identification by XRD of V-, Bi-, and Sb-modified AMPA catalysts

Type of catalyst	Temperature region		Remarks from powder X-ray diffraction patterns
	Appearance of AMPA (°C)	Keggin ion decomposition observed (°C)	
V ₁	300–400	450–500	Cubic structure of AMPA stable up to 400 °C and decomposition starts at 450–500 °C
AMPV ₂	300–350	400–500	Cubic structure of AMPA stable up to 350 °C and decomposition started between 400 and 450 °C
AMPBi ₁	300–400	400–500	Cubic structure of AMPA stable up to 400 °C and decomposition starts between 400 and 450 °C
AMPBi ₂	300–350	400–500	Diffraction lines due to AMPA disappeared at 400 °C, and the lines due to MoO ₃ along with Bi ₉ PMo ₁₂ O ₅₂ were observed
AMPSb ₁	300–350	400–500	Decomposition started at 400 °C and complete decomposition observed in 450–500 °C
AMPSb ₂	300–350	400–500	Decomposition started at 400 °C and complete decomposition observed in 450–500 °C
AMPSb ₃	300–500	400–500	Small diffraction lines of AMPA were observed even at 450 °C

such as (NH₄)₂(VO)₃(P₂O₇)₂, during the course of the reaction. From the comparison of the absorption band appearing at 1,420 cm⁻¹ (corresponding to NH⁴⁺ ion) in both the VOPO₄ catalysts, it seems plausible that the aforesaid ammonium complex formation is more facile in the case of α- than in the β-isomorph.

3.6 V, Sb, and Bi Modified AMPA-Based Systems

The addition of transition metals to heteropoly compounds is an important approach to control their redox properties and improve their thermal stability. Metal can be coordinated with a heteropoly ion in three different ways to form metal coordinated polyions, which show unique catalytic activities for various reactions. A simple combination of metal salts with heteropoly ion is the most commonly used method to prepare the transition metal modified heteropoly compounds. V, Bi, and Sb substituted AMPA catalysts are prepared and the influence of their physicochemical properties on ammoxidation functionality determined. The active phases identified by XRD in all the catalysts at calcination temperatures of 300–500 °C are shown in Table 2.3.

Table 2.4 MP conversion on transition metal modified AMPA catalysts at 380 °C

Types of catalyst	Calcination temperature of catalysts				
	300 °C	350 °C	400 °C	450 °C	500 °C
AMPV ₁	62	60	53	50	45
AMPV ₂	50	48	46.2	43.5	35
AMPBi ₁	54	56	60	63.2	66
AMPBi ₂	60	59.6	55.3	51	51.8
AMPSb ₁	50.4	47	45.3	43	40
AMPSb ₂	30	37	43	43.2	72
AMPSb ₃	21	20	25	53	58

Table 2.5 Selectivity to CP (S–CP %) on transition metal modified AMPA catalysts at 380 °C

Types of catalyst	Calcination temperature of catalysts				
	300 °C	350 °C	400 °C	450 °C	500 °C
AMPV ₁	93	90	89	87.3	86.2
AMPV ₂	95	94.5	93.4	91	91.3
AMPBi ₁	87	85	83	81	77
AMPBi ₂	90	85.4	64	80.8	78.9
AMPSb ₁	96	92.5	85.4	84.8	76
AMPSb ₂	96.6	96.8	91.6	87	83
AMPSb ₃	98	98.2	97	94.2	90.6

3.6.1 Influence of Calcination Temperature on the Modified AMPA Catalysts

From the activity results (Tables 2.4 and 2.5), it can be observed that the decrease in conversion at higher calcination temperatures from 450 to 500 °C in the case of V and Bi modified catalysts is due to low thermal stability and decomposition of AMPA at these temperature and could also be due to formation of mixed oxide as observed by the formation of bismuth phosphomolybdate phase. Reverse is the case with AMPSb catalysts which show greater stability to AMPA even at higher calcination temperatures. With increase in calcination temperature from 300 to 500 °C, all AMPSb samples show increase in conversion and a slight decrease in selectivity to CP. This fact can be explained by taking the hypothesis proposed by Cavani et al. [64] that with increase in calcination temperature, the amount of ammonia expelled out from the secondary structure is more and the amount of antimony going into the secondary structure will increase. It is known that, due to the redox reaction between the $[\text{PMo}_{12}\text{O}_{40}]^{3-}$ and the residual Sb^{3+} ions, the oxidation state of Mo reduces from 6 to 5. The extent of reduction is directly proportional to the antimony content. From this discussion, we can say that the sample AMPSb₃ has more amount of Mo^{5+} species. The presence of reduced molybdenum species (Mo^{5+}), which are known to be more active in redox-type reactions, is the reason for high conversions and yield of CP.

3.6.2 Influence of the Number of Transition Metal Atoms Incorporated to AMPA

Incorporation of one V metal atom, which goes into the primary structure of Keggin ion of AMPA catalyst leads to enhancement of the redox properties of the catalysts. However, addition of further V may lead to the formation of amorphous material like $[\text{VO}]^{2+}$ species in the secondary structure, which also helps enhance the redox behavior of the catalysts. However, the addition of two V atoms leads to lower thermal stability of the cubic secondary structure of AMPA catalysts possibly due to replacement of ammonium cations by other vanadium oxo species.

Addition of one Bi atom enhances the thermal stability of the AMPA catalysts contrary to the general observation that the addition of guest metal reduces the thermal stability of the parent compound by formation of lacunary species. But in the present case, better thermal stability can be attributed to interaction between Mo-Bi species. Further, the addition of Bi in place of two molybdenum atoms in the Keggin ion leads to formation of bismuth phosphomolybdate during the preparation of catalyst with a consequent decrease in the formation of AMPA. The formation of this new species reduces the selectivity to CP considerably.

Addition of one Sb atom leads to a dramatic increase in thermal stability in AMPA catalysts. In general, the AMPA decomposes into its oxides at temperature between 400 and 450 °C, but the addition of three Sb atoms leads to existence of AMPA even after calcination at 450 °C revealing the enhanced thermal stability. This effect can be attributed to a partial replacement of (NH_4^+) by Sb metal atoms. When compared with AMPA, the Sb-modified catalysts show lower activity. Reduced ammonium content in the secondary structure, with addition of Sb, seems to be the reason for the decreased activity. But there is considerable improvement in the CP selectivity. This can be attributed to the redox reaction between the $[\text{PMo}_{12}\text{O}_{40}]^{3-}$ and the residual Sb^{3+} ions. The oxidation state of Mo reduces from 6 to 5. The extent of reduction is directly proportional to the antimony content. The presence of reduced molybdenum species (Mo^{5+}) may be responsible for higher selectivity.

3.7 Supported Vanadium Incorporated AMPA Systems

Bulk catalysts have low surface area and thermal stability. Therefore, in order to increase thermal stability and surface area, these catalysts are to be deposited on different supports. Diffusion resistance observed in bulk catalysts can be overcome by dispersed on different supports. An enhancement in the reduction of molybdenum species can be achieved in AMPV because of vanadium incorporation. The thermal stability of supported catalysts is higher than that of the bulk catalysts.

The powder X-ray diffraction patterns (XRD) of fresh AMPV/ TiO_2 catalysts calcined at 350 °C are shown in Fig. 2.24A. Details of the characterization and catalytic activity of all the catalysts can be found in our previous publications [65–67]. The low weight percent catalysts did not reveal any diffraction peaks of

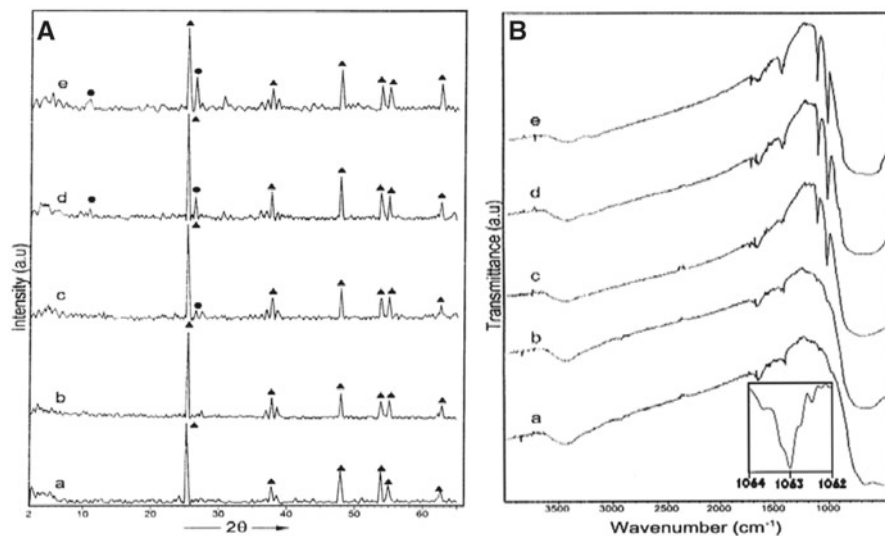
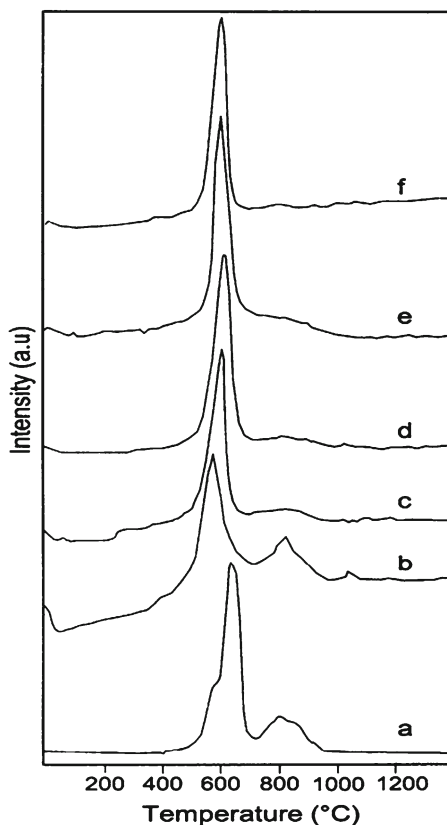


Fig. 2.24 (A) XRD and (B) FTIR spectra of AMPV/TiO₂ catalysts: (a) AMPV-5, (b) AMPV-10, (c) AMPV-15, (d) AMPV-20, and (e) AMPV-25; (●) Keggin ion (▲) TiO₂ (Ref. [65])

crystalline AMPV. They exhibited mainly the patterns of titania support. This might be due to well dispersion of Keggin units on titania surface. The hydroxyl groups bonded to the titania surface are protonated in the acidic solution thereby creating positively charged surface hydroxyl groups. These groups can bind a complex anion like that of the Keggin $[\text{PMo}_{12}\text{O}_{40}]^{3-}$ ion by electrostatic attraction leading to strong interaction of the AMPV with the support surface. Such an opinion is also expressed by Bruckman et al. [68]. The XRD peaks of the Keggin ion [69] are visible for the catalysts with 20 wt% of AMPV or higher. These catalysts show crystalline patterns of the salt. The intensities of the two main peaks corresponding to the salt have increased with increase in AMPV loading. It is also further confirmed with the FTIR spectra of AMPV supported on titania samples shown in Fig. 2.24B. The IR spectra show bands at 1,410, 1,065, 960, 873, and 786 cm^{-1} assigned to stretching vibrations of NH_4^+ ion, (P–O_d), (Mo–O_i), (Mo–O_b–Mo), and (Mo–O_c–Mo), respectively [7]. The peak obtained at 1,065 cm^{-1} is resolved using a resolution of 0.1 cm^{-1} , and it is shown in the inset of Fig. 2.24B; the splitting of P–O_a band at 1,065 cm^{-1} can be observed. It is known that the introduction of a metal other than Mo in the Keggin ion induces a decrease in the Mo–O_d stretching frequencies and a possible splitting of the P–O_a band [48]. This splitting suggests the incorporation of V into the Keggin ion. These data suggest that the Keggin structure has been formed on titania during the synthesis. The intensity of the peaks related to Keggin ion are weak at lower loading but show an increase trend with increasing loading, similar to the observations made in the case of XRD.

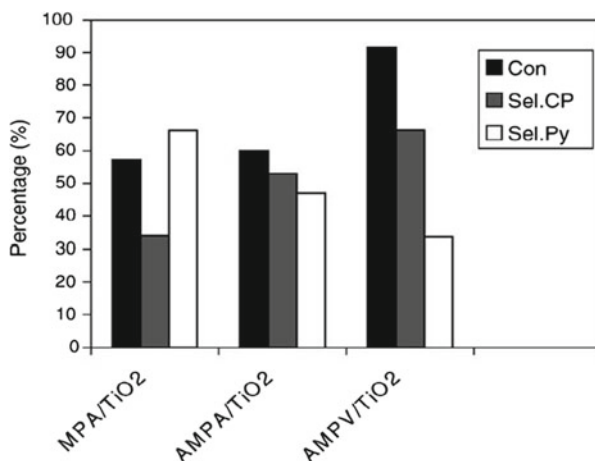
TPR measurements on the catalysts have shown (Fig. 2.25) that the main reduction peak of HPCs are within the temperature range of 650–730 °C. The reduction peaks

Fig. 2.25 TPR profiles of AMPV/TiO₂ catalysts: (a) support, (b) AMPA-5, (c) AMPA-10, (d) AMPA-15, (e) AMPA-20, (f) AMPA-25



in the 650–730 °C range may be ascribed to the reduction of free metal oxides originating from the decomposition of Keggin oxoanion, whereas the reduction peaks below 540 °C can be ascribed to the reduction of transition metal cations in the framework structure of HPCs [48, 70–73]. The TPR pattern of the unsupported bulk AMPV catalyst is also included for comparison. The bulk AMPV catalyst shows three distinct reduction temperatures at 613, 658, and 821 °C. The first two peaks may be due to reduction of more than one oxomolybdenum species. The high-temperature reduction peak, however, can be ascribed to the reduction of bulk MoO₃ formed at high temperatures and/or reduction of new phase containing V and P [72]. In contrast, the titania-supported AMPV catalysts exhibit only one reduction temperature maximum around 575–595 °C, which can be attributed to the reduction of octahedrally coordinated Mo⁶⁺ polymolybdates to a lower valence state. In the supported catalysts, the shift in the principal TPR peak indicates that the reduction of molybdenum species is enhanced due to more interaction of AMPV with titania. Sainero et al. [73] also observed a low-temperature shift in TPR peak when an interacting support like zirconia is added to silica in the case of supported MPA catalysts. As loading increases, the reduction temperature shifts to higher temperature.

Fig. 2.26 Activity patterns of the various catalysts during the ammoxidation of MP: MPA/TiO₂, AMPA/TiO₂, and AMPV/TiO₂ catalysts (Ref. [65])



3.7.1 Comparison of the Catalytic Activity of Titania-Supported Bulk, Ammonium Salt, and Modified Ammonium Salt

In order to determine the effect of vanadium substitution for molybdenum in the ammoxidation reaction, ammoxidation of MP was studied on titania-supported MPA, the unsubstituted AMPA (of 20 wt% loading), and the AMPV catalysts. The results obtained over these catalysts are shown in Fig. 2.26. The titania-supported AMPV catalyst shows better activity than the other two catalysts. The performance of the catalysts is in the following order: AMPV > AMPA > MPA. The MPA catalyst leads to formation of an undesired dealkylation product, pyrazine. The conversion of acid (MPA) to its ammonium salt (AMPA) improves the formation of CP, a desired product, by reducing the pyrazine selectivity to some extent. However, incorporation of vanadium into AMPA leads to substantial improvement in the selectivity toward CP, by minimizing the formation of pyrazine with high conversion of MP.

The conversion of MP and acidity of the catalyst are in good agreement. As can be seen from an example shown in Fig. 2.27, the conversion obtained at 420 °C is proportional to the acidity on AMPV/CeO₂ catalysts. Conversion of MP at 380 °C and acidity values are tabulated and shown in the Table 2.6. The conversion and acidity values increase as the AMPV loading increases up to 20 wt%. Further increase to 25 wt% decreases the conversion of MP and the acidity, except in AlF₃-supported catalysts. All the supported systems have shown 10–15 % difference in their conversion and negligible selectivity to CP and high selectivity to pyrazine. The conversion of MP to CP is dependent upon the acid strength of the catalyst. The conversion of MP is not proportional to specific surface area of the supported catalysts, possibly due to the contribution from the support. The observation that increasing AMPV loading increases the performance of the catalyst indicates the active role of AMPV. Highly acidic supports like AlF₃ are not favorable, because they react with AMPV and form unwanted salt, which drastically reduce the catalyst

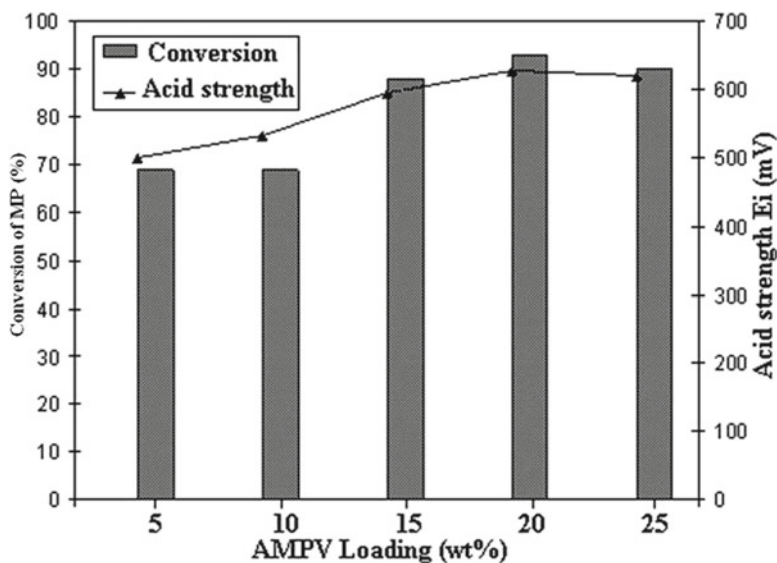


Fig. 2.27 Conversion and acid strength values of AMPV/CeO₂ catalyst at 420 °C (Ref. [67])

Table 2.6 Conversion and selectivity values of 20 % AMPV on different supports at 380 °C (Ref. [67])

Catalyst	Conversion of MP (%)	Selectivity to CP (%)	Acid strength (Ei)
20 %AMPV/AlF ₃	58	50	610
20 %AMPV/ZrO ₂	62	48	458
20 %AMPV/TiO ₂	82	66	591
20 %AMPV/SiO ₂	96	54	730
20 %AMPV/CeO ₂	72	80	628

performance and selectivity to desired product. These supports need higher loading to get the optimum conversion and selectivity. Supports having moderate acidity seem to be best suited for the activity and selectivity of the catalysts. The selectivity of the catalysts obtained at 380 °C is given in Table 2.6. A comparison of the activity and selectivity data obtained on the AMPV/MO (MO-Metal Oxide) catalysts at various temperatures from 360 to 420 °C (not shown here) reveals that the activity and selectivity of different supports vary in the following order; AMPV/CeO₂ > AMPV/SiO₂ > AMPV/TiO₂ > AMPV/ZrO₂ > AMPV/AlF₃. The high activity of ceria-supported catalysts is due to its reducible nature and high oxygen storage capacity of ceria. Therefore, this system is expected to show significant salt-support interaction. All the catalysts have shown considerable amounts of by-product pyrazine at lower loadings, and it is reduced gradually with increased amount of AMPV content in the catalysts.

4 Conclusions

The conclusions are drawn from the above study as follows:

1. AMPA offers higher activity and selectivity compared to its parent acid, MPA, in the ammoxidation of MP. It is possible to tune the catalytic performance of AMPA; by restricting the conversion, the CP selectivity could be maximized to achieve atom-economy. AMPA is thermally more stable than the MPA. Even though these heteropoly compounds decompose into their component oxides during their preparation when subjected to higher calcination temperatures, they get regenerated in the course of reaction. However, at very high calcination temperatures, of the order of 500 °C, AMPA decomposes, at least partially, into non-regenerable, inactive species, thus limiting the maximum temperature of pretreatment.
2. The catalytic activity is not proportional to specific surface area of the supported catalysts, possibly due to the contribution from the support, which is difficult to quantify. The observation that increasing AMPA loading increases the performance of the catalyst dramatically indicates the active role of AMPA. Supports with more number of basic sites like γ -Al₂O₃ are not favorable, because they react with AMPA and form unwanted salt, which drastically reduce the catalyst performance. These supports need higher loading to get the optimum conversion and selectivity. Supports having moderate acidity such as Nb₂O₅, TiO₂, and ZrO₂ seem to be best suited for the activity and selectivity of the catalysts. Supported catalysts with optimum loading of AMPA (between 15 and 20 wt%) on TiO₂ and ZrO₂ offered better MP conversion and CP selectivity than bulk AMPA. The amount of AMPA loading to obtain optimum activity varied with acidity of the supports. Interacted species seems to be responsible for the activity and selectivity as revealed by the ³¹P MAS NMR studies.
3. Addition of one V metal atom, which goes into the primary structure of Keggin ion of AMPA catalyst leads to enhancement of the redox properties of the catalysts. Addition of further V may lead to the formation of amorphous material like [VO]²⁺ species in the secondary structure, which also helps enhance the redox behavior of the catalysts. Addition of two V atoms leads to lower thermal stability of the cubic secondary structure of AMPA catalysts; it may be due to the replacement of ammonium cations by other vanadium oxo species.
4. Addition of one Bi atom enhanced the thermal stability of the AMPA catalysts, contrary to the general observation that the addition of guest metal reduces the thermal stability of the parent compound by formation of lacunary species. But in the present case, better thermal stability could be attributed to interaction between Mo-Bi species. Further addition of Bi corresponding to two molybdenum atoms in the Keggin ion leads to formation of bismuth phosphomolybdate during the preparation of catalyst with a consequent decrease in the formation of AMPA. The formation of the new species reduced the selectivity to CP considerably.
5. Addition of Sb metal atom leads to a dramatic increase in thermal stability in AMPA catalysts. In general, the AMPA decomposes into its oxides at temperature between 400 and 450 °C, but the addition of three Sb atoms leads to existence of

AMPA even after calcination at 450 °C revealing the enhanced thermal stability. This effect can be attributed to a partial replacement of (NH₄⁺) by Sb metal atoms. When compared with AMPA, the Sb-modified catalysts show lower activity. Reduced ammonium content in the secondary structure, with addition of Sb, seems to be the reason for reduced activity. But there is considerable improvement in the CP selectivity. This can be attributed to the redox reaction between the [PMo₁₂O₄₀]³⁻ and the residual Sb³⁺ ions. The oxidation state of Mo reduces from 6 to 5. The extent of reduction is directly proportional to the antimony content. The presence of reduced molybdenum species (Mo⁵⁺) may be responsible for higher selectivity. The catalytic performance of the transition metal incorporated AMPA catalysts is in the order of AMPSb ≥ AMPV > AMPBi.

6. V incorporated MPA catalysts offered better catalytic performance than the bulk MPA and supported MPA, probably due to increase in redox properties of the VMPA catalyst. We obtained superior catalytic activity for the VMPA supported on TiO₂ catalysts, which could be related to fine dispersion of catalytically active HPA clusters on the support.
7. In situ synthesis of AMPA on the surface of metal phosphates is advantageous by several means. This protocol has been established by synthesizing AMPA supported on NbOPO₄, FePO₄, and VOPO₄ (α and β forms). At optimum MoO₃ loading (between 15 and 20 wt%) of polyatom (Mo), the catalysts offered more catalytic activity than the simple impregnated supported AMPA catalysts. The conversion rate and yield of CP are varied with physicochemical properties of the metal phosphate. NbOPO₄ and VOPO₄ offered high conversion of MP. FePO₄ offered less conversion but high selectivity to CP than NbOPO₄ and VOPO₄.
8. FTIR technique can be used to determine the dispersion of AMPA on supports.

Acknowledgments Thanks are due to Director, CSIR-Indian Institute of Chemical Technology, Hyderabad, for permitting to carry out the work. The authors are thankful to Dr. I Suryanarayana for his help in the interpretation of NMR results.

References

1. Wiberg KB (ed) (1995) Oxidation in organic chemistry. Academic, New York
2. Moffat JB (2001) Metal-oxygen clusters. The surface and catalytic properties of heteropoly oxometalates. Kluwer Publications, New York
3. Misono M (1987) Catal Rev Sci Eng 29:269
4. (a) Hill CL (ed) (1998) Chem Rev 98:1; (b) Okuhara T, Mizuno N, Misono M (1996) Adv Catal 41:113
5. Inamaru K, Ono A, Kubo H, Misono M (1998) J Chem Soc Faraday Trans 97:1765
6. Martin A, Lucke B (2000) Catal Today 57:61
7. Bondareva VM, Andrushkevich TV, Detushera LG, Latvak GS (1996) Catal Lett 42:113
8. (a) Keggin JF (1933) Nature 131:908; (b) Wells AF (1945) Structural inorganic chemistry. Oxford University Press, Oxford, p 344; (c) Dawson B (1953) Acta Crystallogr 6:113; (d) Anderson JS (1937) Nature 140:850
9. Pope MT (1983) Heteropoly and isopoly oxometalates. Springer, Berlin/New York
10. (a) Mc Garvey GB, Moffat JB (1991) J Catal 130:483; (b) Hu J, Burns RC (2000) J Catal 195:360
11. Knoth WH, Harlow RL (1981) J Am Chem Soc 103:1856

12. Misono M, Nojiri N (1990) *Appl Catal* 64:1
13. Ahmed S, Moffat JB (1988) *Appl Catal* 40:101
14. Faraj M, Hill CL (1987) *J Chem Soc Chem Commun* 1487
15. Kozhevnikov IV, Matveev KI (1983) *Appl Catal* 5:135–150
16. Keana JFW (1986) *J Am Chem Soc* 108:7951
17. (a) Buzt T, Vogdt C, Lerf H, Knozinger H (1989) *J Catal* 116:31; (b) Smit JVR (1958) *Nature* 181:1530; (c) Guilbault GG, Brignac PJ (1971) *Anal Chim Acta* 56:139; (d) Seidle AR, Newmark RA, Gleason WB, Skarjune RP, Hodgson KO, Rol RA, Day VB (1988) *Solid State Ionics* 26:109
18. Mizuno N, Misono M (1998) *Chem Rev* 98:199
19. Marchal-Roch C, Bayer R, Moison FF, Teze A, Herve G (1996) *Top Catal* 3:407
20. (a) Cavani F, Etienne E, Favaro M, Falli A, Trifiro F, Hecquet G (1995) *Catal Lett* 32:215; (b) Knapp C, Ui T, Nagai K, Mizuno N (2001) *Catal Today* 71:111
21. Centi G, Perathoner S (1998) *Catal Rev Sci Eng* 40:175
22. Kozhevnikov IV (1997) *J Mol Catal A Chem* 111:109
23. Ressler T, Timpe O, Girgsdies F, Wienold J, Neisius T (2005) *J Catal* 231:279
24. Liu H, Iglesia E (2003) *J Phys Chem B* 107:10840
25. Liu H, Iglesia E (2004) *J Catal* 223:161
26. Mestl G, Ilkenhans T, Spielbaur D, Dieterle M, Timpe O, Krohnert J, Jentoft F, Knozinger H, Schlögl R (2001) *Appl Catal A Gen* 210:13
27. Kozhevnikov IV (1997) *J Mol Catal A* 117:151
28. Berzelius J (1826) *Pogg Ann* 6:369
29. McGarvey GB, Moffat JB (1991) *J Catal* 132:100
30. Bielanski A, Malecka A, Kubelkova L (1989) *J Chem Soc Faraday Trans* 85(9):2847
31. Rao KM, Gobetto R, Innibello A, Zacchina A (1989) *J Catal* 119:512
32. Kozhevnikov IV (1995) *Catal Rev Sci Eng* 37(2):311
33. Nowinska K, Fiedorow R, Adamiec J (1991) *J Chem Soc Faraday Trans* 87:749
34. Lapham D, Moffat JB (1991) *Langmuir* 7:2273
35. Ito T, Irumaru K, Misono M (2001) *Chem Mater* 13:824
36. Lingaiah N, Mohan Reddy K, Nagaraju P, Sai Prasad PS, Wachs IE (2008) *J Phys Chem C* 112:8294
37. Li X-K, Zhao J, Ji W-j, Zhang Z-B, Chen Y, Chak-Tong A, Han S, Hibst H (2006) *J Catal* 237:58
38. Sopa M, Waclaw-Held A, Grossy M, Pijanka J, Nowinska K (2005) *Appl Catal A Gen* 285:119
39. Garte JH, Hamm DR, Mahajan S (1994) In: Pope MT, Muller A (eds) *Polyoxometalates: from platonic solids to anti-retroviral activity*. Kluwer Academic Publisher, Dordrecht/Boston, p 281
40. Narasimha Rao K, Gopinath R, Sai Prasad PS (2001) *Green Chem* 3:20
41. Marchal-Roch C, Laronze N, Guillou N, Teze A, Herve G (2000) *Appl Catal A Gen* 199:33
42. Rao KN, Gopinath R, Hussain A, Lingaiah N, Sai Prasad PS (2000) *Catal Lett* 68:223
43. Albonetti S, Cavani F, Trifiro F, Gazzano M, Koutyrev M, Aissi FC, Aboukais A, Guelton M (1994) *J Catal* 146:491
44. Damyanova S, Cubeiro ML, Fierro JLG (1999) *J Mol Catal A Chem* 142:85; Damyanova S, Fierro JLG (1998) *Chem Mater* 10:876
45. Hodnett BK, Moffat JB (1984) *J Catal* 88:253
46. Tsigdinos GA (1974) *Ind Eng Chem Prod Res Dev* 13:267
47. McMonagle JB, Moffat JB (1985) *J Catal* 91:132
48. Rocchiccioli-Deltcheff C, Fournier M (1991) *J Chem Soc Faraday Trans* 87:3913
49. Van Veen JAR, Sudmeijer O, Emeis CA, de Wit H (1986) *J Chem Soc Dalton Trans* 1825–1831
50. Iwamoto R, Fernandez C, Amoureux JP, Grimblot J (1998) *J Phys Chem B* 102(22):4343
51. Damyanova S, Fierro JLG, Sobrados I, Sanz J (1999) *Langmuir* 15:469
52. Essayen N, Frety R, Coudurier G, Vedrine JC (1997) *J Chem Soc Faraday Trans* 93(17):3243
53. Nowinska K, Kaleta W (2000) *Appl Catal A Gen* 203:91
54. Black JB, Clayden NJ (1984) *J Chem Soc Dalton Trans* 2765
55. Kraus H, Prins R (1996) *J Catal* 164:251

56. Narasimha Rao K, Gopinath R, Santhosh Kumar M, Suryanarayana I, Sai Prasad PS (2001) *Chem Commun* (2088)
57. Narasimha Rao K, Mohan Reddy K, Lingaiah N, Suryanarayana I, Sai Prasad PS (2006) *Appl Catal A Gen* 300:139
58. Srilakshmi Ch, Narasimha Rao K, Lingaiah N, Suryanarayana I, Sai Prasad PS (2002) *Catal Lett* 83:3
59. Srilakshmi Ch, Lingaiah N, Suryanarayana I, Sai Prasad PS, Ramesh K, Anderson BG, Niemantsverdriet JW (2005) *Appl Catal* 296:54
60. Srilakshmi Ch, Lingaiah N, Nagaraju P, Sai Prasad PS, Kalevaru V, Narayana A, Martin A, Lucke B (2006) *Appl Catal* 309:247
61. Srilakshmi Ch, Nagaraju P, Sreedhar B, Sai Prasad PS, Narayana Kalevaru V, Lucke B, Martin A (2009) *Catal Today* 141:337
62. Srilaxmi C, Lingaiah N, Hussain A, Sai Prasad PS, Narayana KV, Martin A, Lucke B (2004) *Catal Commun* 5:199
63. Rocchiccioli-Deltcheff C, Aouissi A, Bettahar MM, Launay S, Fournier M (1996) *J Catal* 164:16
64. Albonetti S, Cavani F, Trifiro F, Koutrev M (1995) *Catal Lett* 30:253
65. Mohan Reddy K, Lingaiah N, Rao KN, Nilofer R, Sai Prasad PS, Suryanarayana I (2005) *Appl Catal A Gen* 296:108
66. Mohan Reddy K, Lingaiah N, Nagaraju P, Sai Prasad PS, Suryanarayana I (2008) *Catal Lett* 122:314
67. Mohan Reddy K, Lingaiah N, Rao PSN, Nagaraju P, Sai Prasad PS, Suryanarayana I (2009) *Catal Lett* 130:154
68. Bruckman K, Che M, Haber J, Tatibouet JM (1994) *Catal Lett* 25:225
69. Marchal-Roch C, Laronze N, Villanneau R, Guillou N, Teze A, Herve G (2000) *J Catal* 190:173
70. Mizuno N, Sun DJ, Han W, Kudo T (1996) *J Mol Catal A Chem* 114:309
71. Dimitratos N, Védrine JC (2003) *Appl Catal A Gen* 256:251
72. Spojakina AA, Kostova NG, Sow B, Stamenova MW, Jiratova K (2001) *Catal Today* 62:315
73. Gomez Sainero LM, Damyanova S, Fierro JLG (2001) *Appl Catal A Gen* 208:63

Environmentally Benign Catalysts

For Clean Organic Reactions

Patel, A. (Ed.)

2013, X, 263 p. 205 illus., 148 illus. in color.,

ISBN: 978-94-007-6710-2